SUPPLEMENTAL DATA
Title: Enhancing Glycolysis Attenuates Parkinson's Disease in Models and Clinical Databases

Figure S1

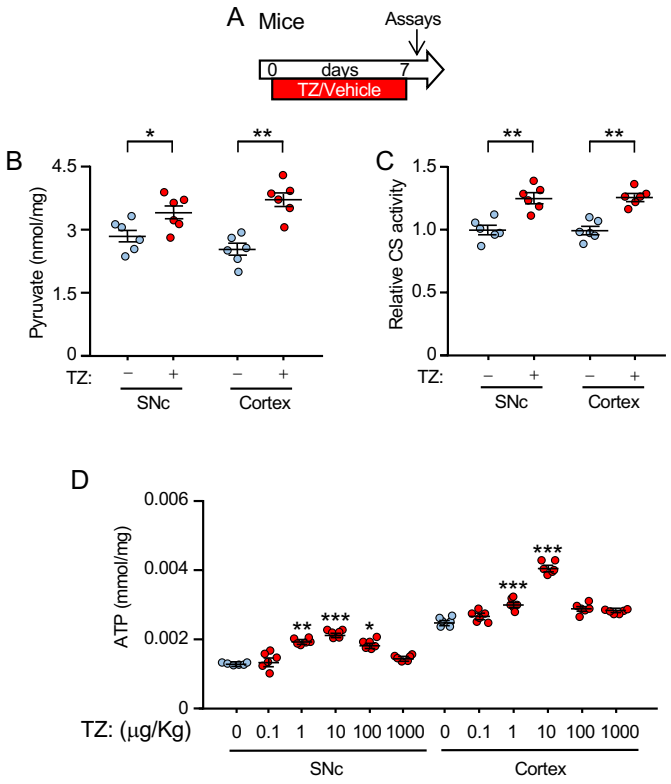

Figure S1. TZ enhances glycolysis and mitochondrial function in vivo in mouse brain.
In all figures, data points are from individual mice, rats, or groups of flies. Bars and whiskers indicate mean±SEM. Blue indicates controls and red indicates TZ treatment. Table S3 shows statistical tests and P values for all comparisons. In the figures, *p<0.05, **p<0.01, ***p<0.001.

A) Schematic for experiments in panels **B-D**. Eight week-old C57bl/6 mice were given TZ (10 µg/kg) or vehicle and were injected i.p. once a day for one week. Assays were at day 7. Samples are from the same animals shown in Figure 1C-1E.

B-D) Pyruvate levels **(B)**, citrate synthase (CS) activity **(C)**, and ATP levels **(D)** measured in mouse SNc and cortex. In panel D, TZ doses are indicated. N=6.

Statistical comparison is *vs*. 0 TZ.

Figure S2

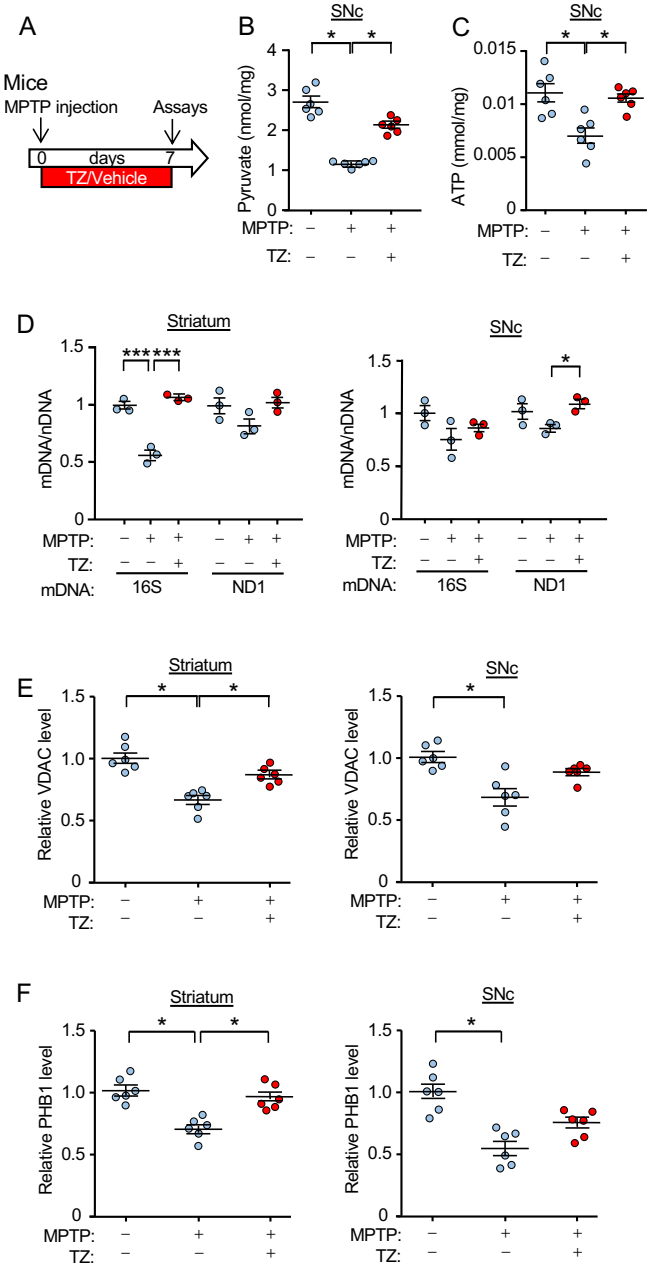

Figure S2. TZ decreases MPTP-induced reductions in glycolysis, ATP levels, and mitochondrial defects in mice.

A) Schematic of experiments in panels **B-F**. C57BL/6 mice (8 week-old) received 4 i.p. injections of MPTP (20 mg/kg at 2 hr intervals) or vehicle on day 0. Mice were then injected with TZ (10 μg/kg) or vehicle (0.9 % saline) once a day for one week and assays were performed on day 7. Samples are from the same animals shown in Figure 2E,2F.

B,C) Pyruvate and ATP levels in mouse SNc. N=6.

D) Mitochondrial DNA (mDNA, *16S* and *ND1*) relative to nuclear DNA (nDNA, intron *β-globin*) by quantitative PCR of mouse striatum and SNc. N=3.

E,F) VDAC **(E)** and PHB1 **(F)** protein levels in striatum and SNc assayed by western blot and normalized to control. N=6.

Figure S3

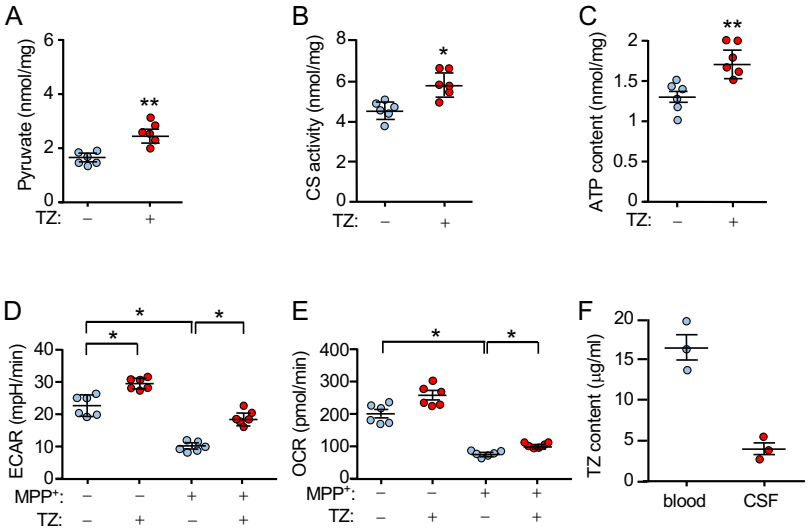

Figure S3. TZ enhances glycolysis and mitochondrial function in M17 human neuroblastoma cells.

A-C) M17 cells were treated with TZ (10 µM) or vehicle. Pyruvate levels **(A)**, citrate synthase (CS) activity **(B)**, and ATP levels **(C)** were measured 24 hr later. N=6.

D-E) M17 cells were treated for 24 hr with vehicle or the MPTP metabolite, 1-methyl-4-phenylpyridinium (MPP^+), which inhibits mitochondrial complex I respiration. They also received TZ (10 µM) or vehicle. Basal extracellular acidification rate (ECAR), a measure of glycolysis **(D)**, and basal O_2 consumption rate (OCR), a measure of mitochondrial respiration **(E)**, were measured 24 h after TZ treatment. N=6.

F) TZ levels in blood and cerebral spinal fluid. TZ was injected i.p. at 30 mg/kg. Blood and cerebrospinal fluid were collected 20 min. later. TZ was quantified by HPLC-ECD. This dose of TZ is substantially higher than that used to activate glycolysis; we used that dose in order to readily detect TZ in the blood and cerebral spinal fluid. Although the mice appeared healthy with this dose, we cannot exclude some adverse effect. N=3.

Figure S4

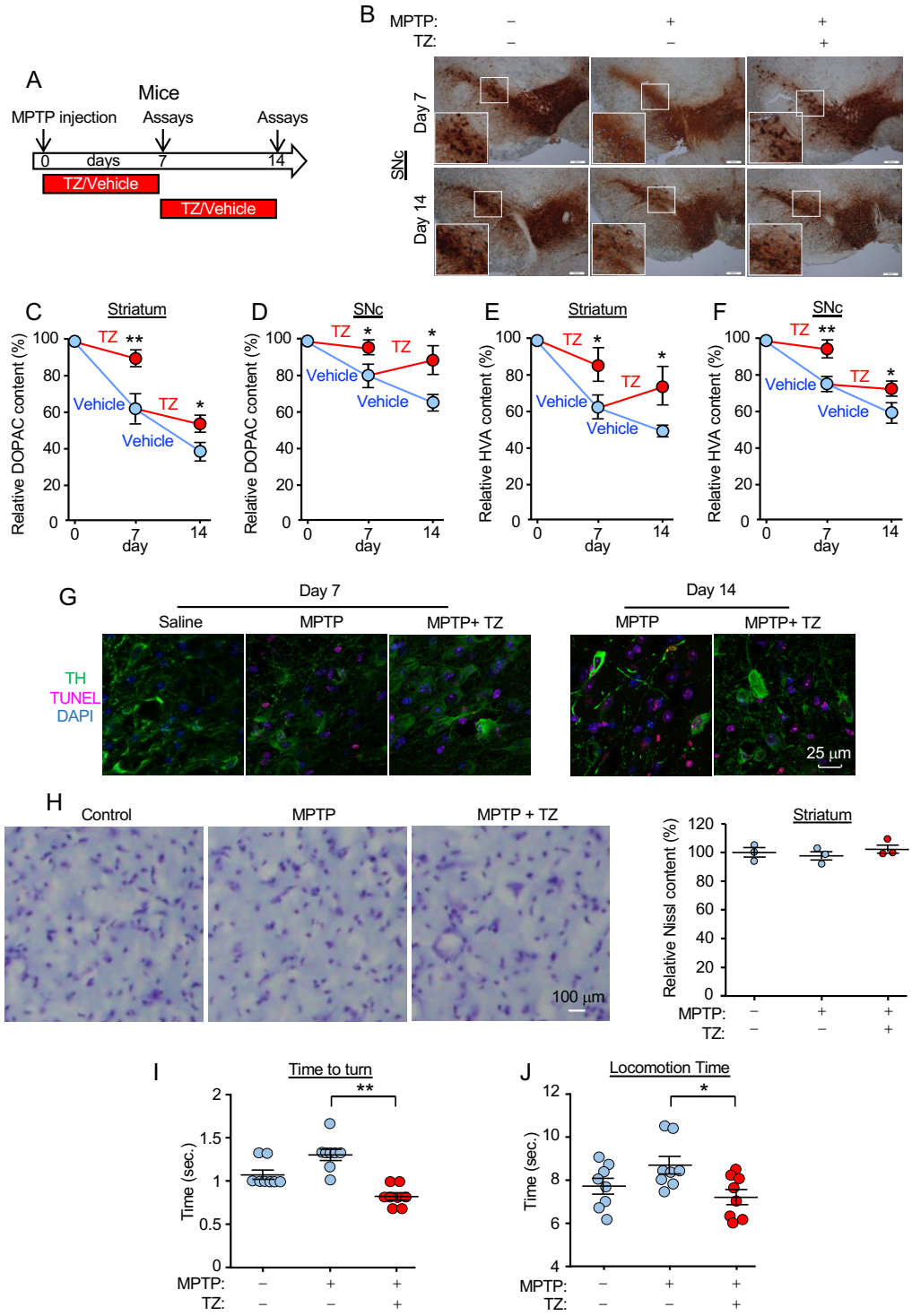
A
Mice
MPTP injection
Assays
Assays
0
days
7
14
TZ/Vehicle
TZ/Vehicle
B
MPTP:
TZ:
Day 7
Day 14
SNc
C
Striatum
Relative DOPAC content (%)
TZ
Vehicle
day
D
SNc
Relative DOPAC content (%)
E
Striatum
Relative HVA content (%)
F
SNc
Relative HVA content (%)
G
Day 7
Day 14
Saline
MPTP
MPTP+ TZ
TH
TUNEL
DAPI
25 μm
H
Control
MPTP
MPTP + TZ
100 μm
Striatum
Relative Nissl content (%)
I
Time to turn
Time (sec.)
J
Locomotion Time
Time (sec.)

Figure S4. TZ attenuated TH-positive neuron death and improved function in an MPTP mouse model.

A) Schematic for experiments in panels **B-J**. C57BL/6 mice (8 week-old) received 4 i.p. injections of MPTP (20 mg/kg at 2 hr intervals) or vehicle on day 0. Mice were then injected with TZ (10 μg/kg) or vehicle (0.9 % saline) once a day for one week and assays were performed on day 7. Other mice began receiving daily TZ or vehicle injections beginning on day 7 and assays were performed on day 14. Protocol is same as shown in Figure 2.

B) Example of TH immunostaining in the SNc on days 7 and 14. Inset shows areas that are shown in Figure 2E. Scale bar, 500 μm.

C-F) Measurement of DOPAC in mouse striatum **(C)** and SNc **(D)** and measurement of HVA in striatum **(E)** and SNc **(F)**. (N=6).

G) Example of TH and TUNEL co-staining in the SNc. TH (green), TUNEL (red), and DAPI (nuclei, blue). Scale bar, 25 μm. Quantitative data are in Figure 2J.

H) Left panels are Nissl staining of neurons in the striatum. Samples were obtained 7 days after MPTP injection. Right panels show the quantification. Results showed no reduction of total number of neurons in the striatum after MPTP injection, indicating lack of substantial cell death except in dopamine neurons. Scale bar, 400 μm. N=3 per group.

I,J) Behavioral response of mice in the pole test. **(I)** Time mice took to turn their heads from upward to downward. **(J)** Time mice took to climb down the pole. N=8.

Figure S5

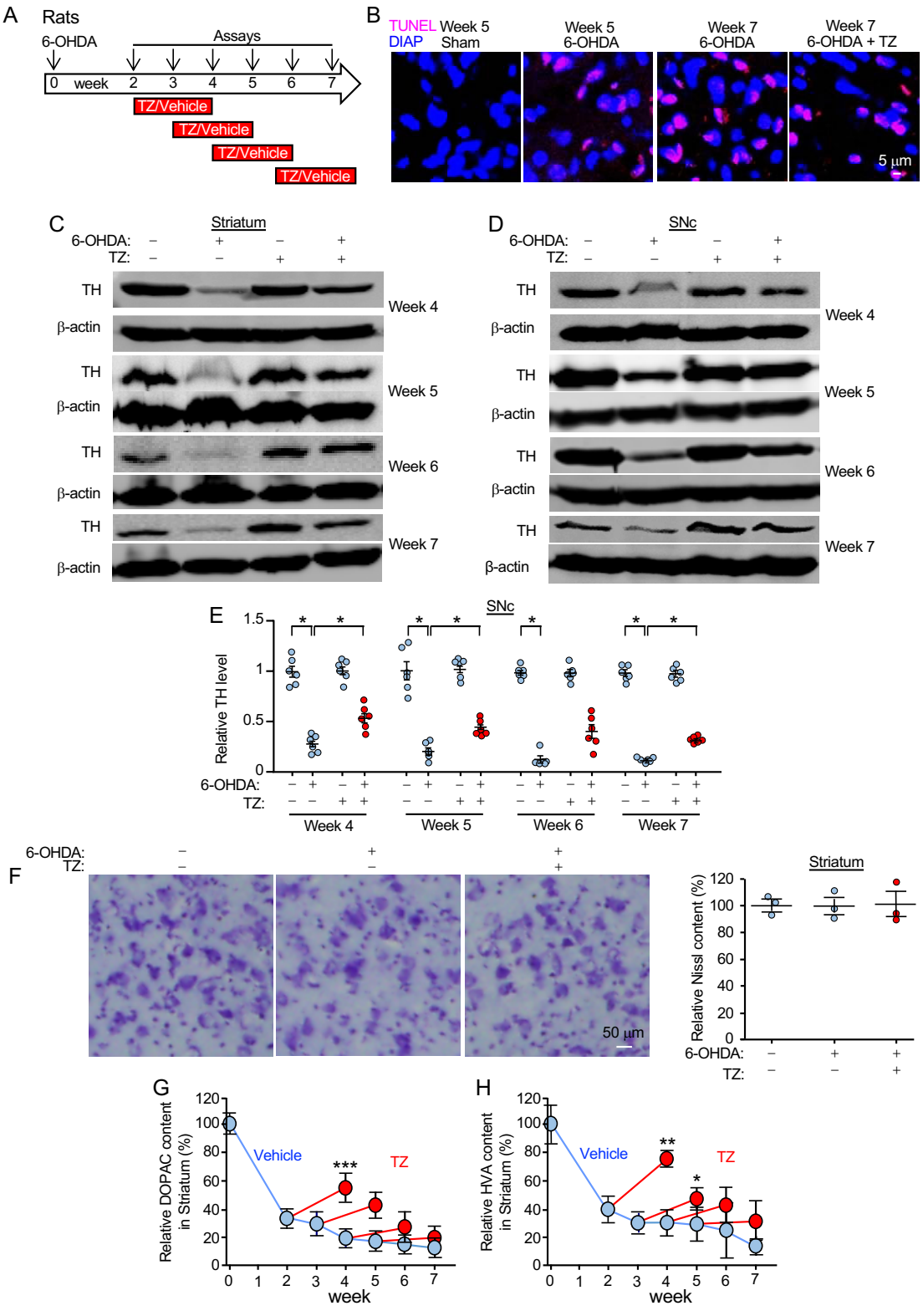
A
Rats
6-OHDA
Assays
0 week 2 3 4 5 6 7
TZ/Vehicle
TZ/Vehicle
TZ/Vehicle
TZ/Vehicle
B
TUNEL
DIAP
Week 5 Sham
Week 5 6-OHDA
Week 7 6-OHDA
Week 7 6-OHDA + TZ
5 μm
C
Striatum
6-OHDA:
TZ:
TH
β-actin
Week 4
Week 5
Week 6
Week 7
D
SNc
E
SNc
Relative TH level
Week 4
Week 5
Week 6
Week 7
F
50 μm
Striatum
Relative Nissl content (%)
G
Relative DOPAC content in Striatum (%)
Vehicle
TZ
week
H
Relative HVA content in Striatum (%)
Vehicle
TZ
week

Figure S5. TZ attenuates neurodegeneration, increases TH and dopamine, and improves motor function when administered after the onset of deterioration.

A) Schematic for experiments in panels **B-H**. 6-OHDA (20 μg) was injected into right striatum of rats on day 0. TZ (70 μg/kg) or saline were injected (i.p.) daily for 2 weeks, beginning 2, 3, 4, or 5 weeks after 6-OHDA injection. Assays were at 0 and 2-7 weeks. Protocol is same as shown in Figure 3.

B) Example of TUNEL staining in the SNc of rat brain. Samples were obtained at 5 weeks in sham-treated animals, 5 weeks in animals that received 6-OHDA, and at 7 weeks in animals that received vehicle or TZ from week 5 to 7. TUNEL (red) and DAPI (nuclei, blue). Scale bar, 5 μm.

C-E) Examples of western blots of TH and β-actin (protein loading control) in the striatum **(C)** and SNc **(D)**. **(E)** shows quantification for SNc; quantification for striatum is in Figure 3C.

F) Nissl staining of neurons in the striatum region. Samples were obtained 2 weeks after 6-OHDA injection. Right panels show the quantification. Results showed no obvious reduction of total number of neurons in the striatum, indicating lack of substantial cell death except in dopamine neurons. Scale bar, 50 μm. Right panels show the quantification. N=3 per group.

G,H) Measurement of DOPAC (G) and HVA (H) in right striatum relative to left (control) striatum. N=6.

Figure S6

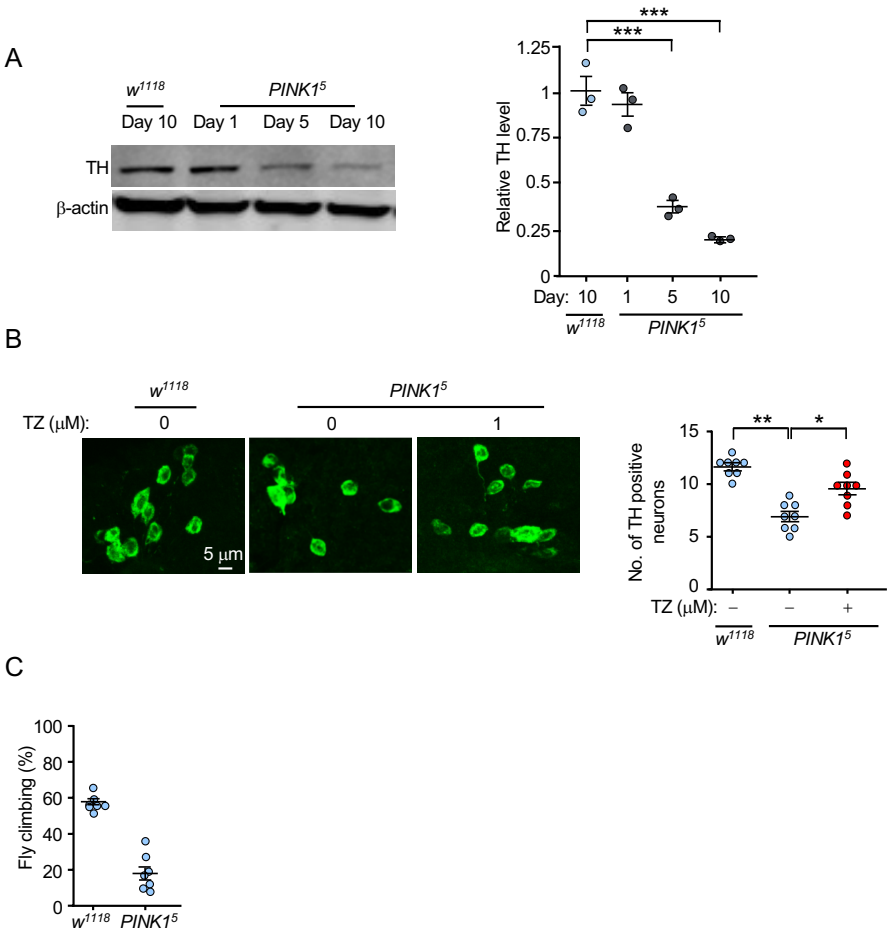

Figure S6. A genetic model of PD in *PINK1*^{5} flies.

A) TH levels in the brain of *PINK1*^{5} flies. Left panel shows example of western blot on the 1st, 5th, and 10th day after hatching. β-actin is protein loading control. Right panel shows quantification. N=3 with 40 fly heads for each treatment in each trial.

B) Immunostaining for TH in *PINK1*^{5} fly brain PPL1 cluster. Left panel shows example of immunostaining for TH. *W*^{1118} flies were used as a genetic background matched control. Quantification of TH neurons is on the right. N=8.

C) Climbing assay for day 1 after eclosion. Note that by day 1 motor performance is already markedly degraded. N=3, with 100 flies for each treatment in each trial.

Figure S7

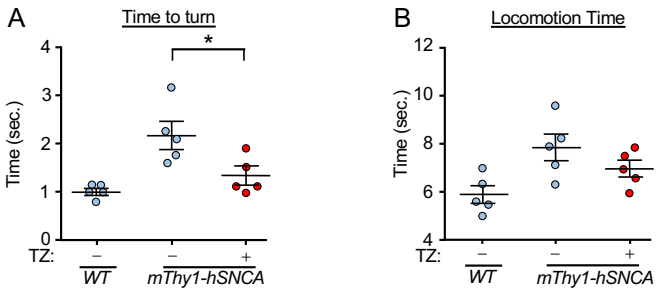

Figure S7. TZ improves motor performance in *mThy-hSNCA* mice
Performance of 15 month-old *mThy1-hSNCA* transgenic mice in the pole test.
A) The time mice took to turn their heads from upward to downward.
B) The time mice took to climb down the pole.
Five mice were tested for each condition.

Figure S8

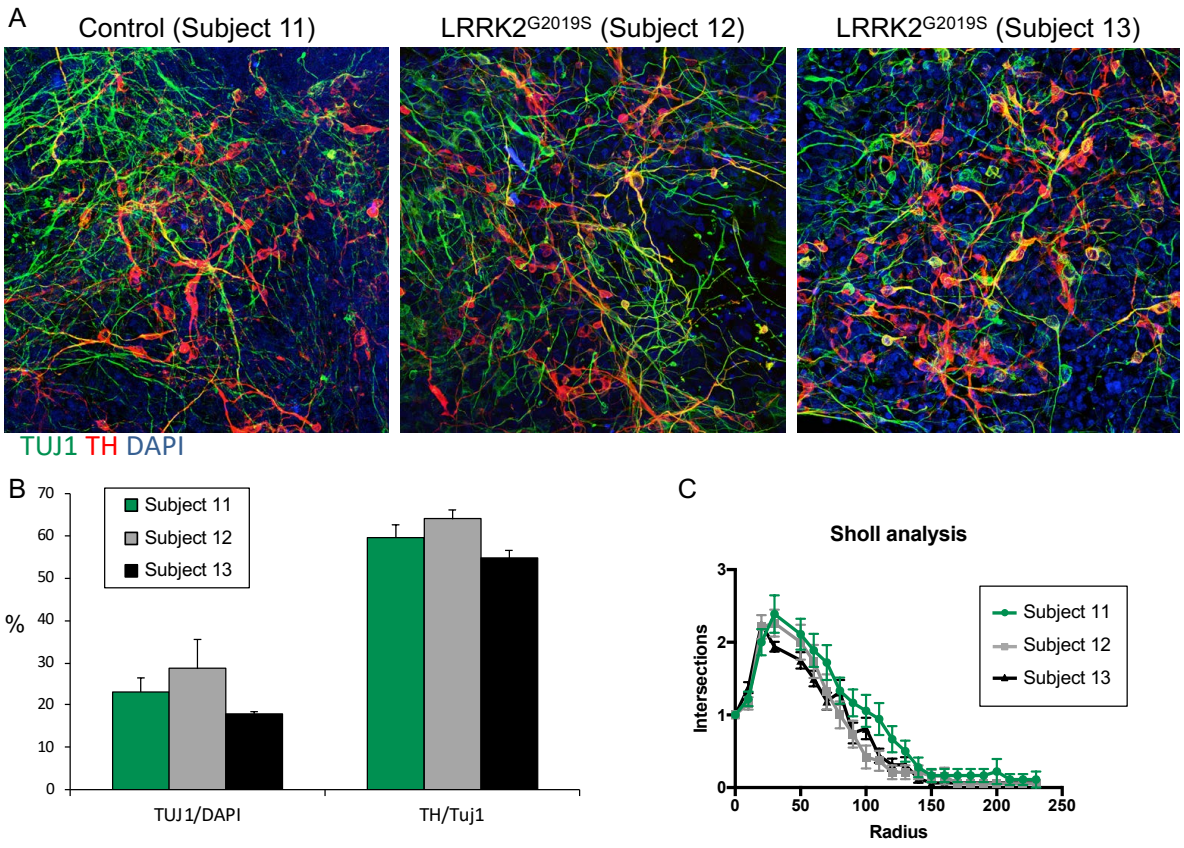

Figure S8. iPSC-derived dopamine neurons from patients with *LRRK2^{G2019S}*.

A) Example of immunofluorescence images of human iPSC-derived DA neurons from a healthy individual (Control, Subject 11), and two independent patients with PD (Subject 12 and 13) carrying the LRRK2G2019S mutation. After 30 days of differentiation, the data showed comparable extents of differentiation and absence of neurodegeneration phenotypes in PD samples. Green labels neuron marker TUJ1, red labels TH, and blue is DAPI (nuclei). Scale bar, 50 μm.

B) Data are the percentage of total neurons (TUJ1/DAPI) and the percentage of neurons that are TH positive (TH/TUJ1).

C) Sholl analysis of TH positive neurons.

Figure S9

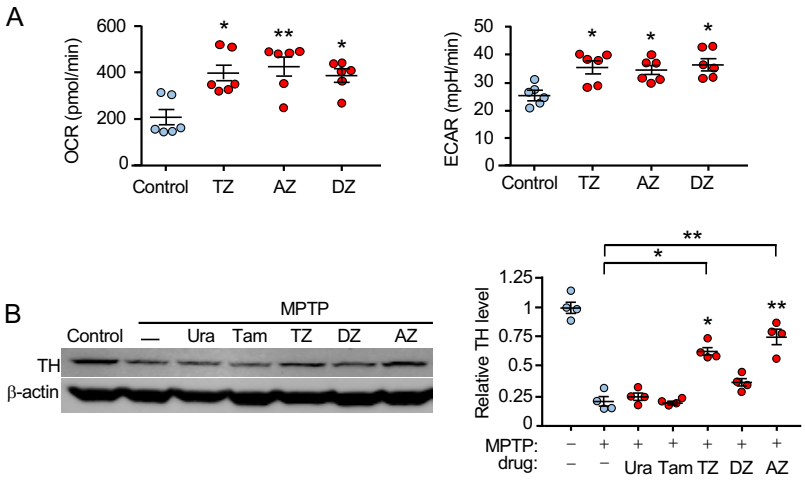

Figure S9. Terazosin, doxazosin, and alfuzosin (TZ/DZ/AZ) enhance glycolysis and mitochondrial function in M17 human neuroblastoma cells and TH levels in MPTP-treated mice.

A) Basal O_2 consumption rate (OCR), a measure of mitochondrial respiration, and basal extracellular acidification rate (ECAR), a measure of glycolysis, were measured 24 hr after adding TZ (10 μM), doxazosin (10 μM), or alfuzosin (10 μM) to M17 human neuroblastoma cells. N=6. Statistical comparisons are to control.

B) Example of western blot of TH and β-actin (protein loading control) in SNc. Quantification is shown on the right. TH protein levels were normalized to the control. Statistical comparisons are to MPTP alone. N=4.

Figure S10

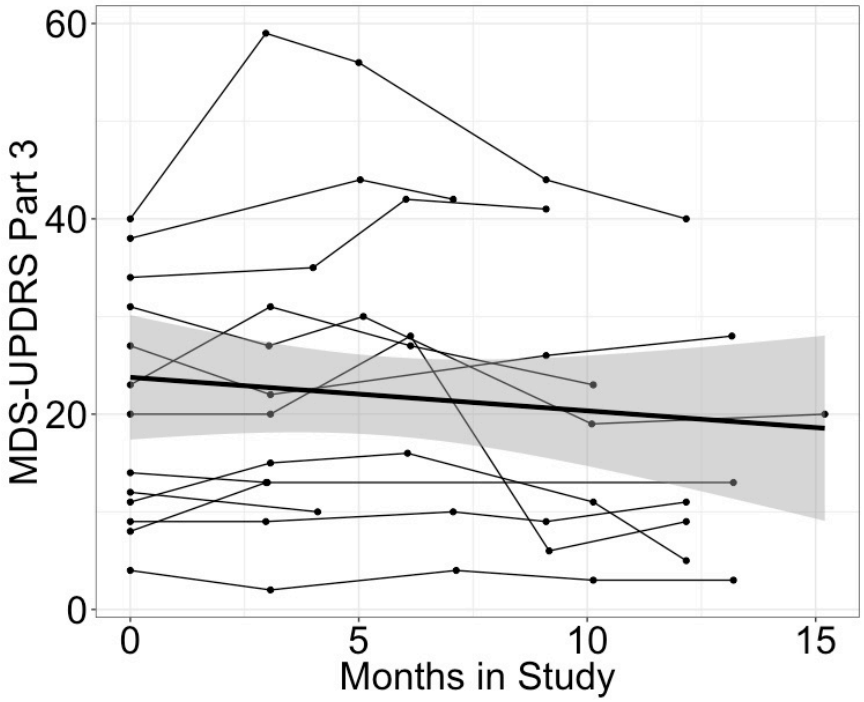

Figure S10. UPDRS scores for 13 patients with PD taking TZ/DZ/AZ.
Each set of data points and lines indicates an individual patient. Bold line and shading indicate the linear regression line and 95% confidence intervals for the 13 patients. See legends of Figure 7 and Table S1 for additional information.

ICD-9 Code	Label	Relative Risk	95% LB	95% UB	P-Value
Motor					
	Walking, gait, coordination				
'333.0'	Other degenerative diseases of the basal ganglia	0.62	0.35	1.11	0.0991
'719.7'	Difficulty in walking	0.74	0.62	0.90	0.0017
'781.0'	Abnormal involuntary movements	0.93	0.79	1.10	0.3958
'781.2'	Abnormality of gait	0.78	0.68	0.89	0.0001
'781.3'	Lack of coordination	0.65	0.49	0.88	0.0038
	Falls				
'920'	Contusion of face, scalp, and neck except eye(s)	0.63	0.47	0.84	0.0013
'959.09'	Injury of face and neck	0.69	0.53	0.90	0.0046
'959.9'	Unspecified site injury	0.62	0.46	0.82	0.0008
'E888.9'	Unspecified fall	0.76	0.61	0.96	0.0165
'V15.88'	History of fall	0.58	0.39	0.87	0.0069
	Essential/Other Tremor				
'333.1'	Essential and other specified forms of tremor	1.23	1.02	1.49	0.026
	Other				
'331.5'	Idiopathic normal pressure hydrocephalus (INPH)	0.71	0.37	1.39	0.3094
'332.1'	Secondary parkinsonism	0.68	0.47	1.00	0.0463
'V57.89'	Care involving other specified rehabilitation procedure	0.73	0.55	0.96	0.0200
Non-Motor					
	Dementia				
'290.0'	Senile dementia, uncomplicated	0.57	0.41	0.78	0.0004
'290.21'	Senile dementia with depressive features	0.30	0.18	0.50	< 0.0001
'294.10'	Dementia in conditions classified elsewhere without behavioral disturbance	0.56	0.42	0.75	0.0001
'294.20'	Dementia, unspecified, without behavioral disturbance	0.56	0.42	0.75	0.0001
'294.21'	Dementia, unspecified, with behavioral disturbance	0.85	0.47	1.53	0.5780
'331.0'	Alzheimer's disease	0.77	0.61	0.97	0.0213
'331.82'	Dementia with lewy bodies	0.46	0.26	0.83	0.0080
'331.83'	Mild cognitive impairment, so stated	0.83	0.57	1.19	0.2920

'780.09'	Other alteration of consciousness	0.72	0.56	0.91	0.0059
'780.93'	Memory loss	1.16	1.01	1.35	0.0375
'780.97'	Altered mental status	0.56	0.44	0.70	< 0.0001
	Neuropsychiatric				
'293.0'	Delirium due to conditions classified elsewhere	0.44	0.23	0.85	0.0122
'293.83'	Mood disorder in conditions classified elsewhere	0.70	0.32	1.51	0.3501
'294.9'	Unspecified persistent mental disorders due to conditions classified elsewhere	0.80	0.53	1.21	0.2824
'296.32'	Major depressive affective disorder, recurrent episode, moderate	0.80	0.50	1.30	0.3582
'296.33'	Major depressive affective disorder, recurrent episode, severe, without mention of psychotic behavior	1.29	0.82	2.04	0.2638
'296.90'	Unspecified episodic mood disorder	0.45	0.18	1.11	0.0769
'298.9'	Unspecified psychosis	0.93	0.70	1.23	0.5858
'300.00'	Anxiety state, unspecified	0.67	0.49	0.92	0.0104
'300.02'	Generalized anxiety disorder	0.92	0.55	1.53	0.7475
'780.02'	Transient alteration of awareness	0.69	0.54	0.88	0.0024
'780.1'	Hallucinations	0.67	0.46	0.99	0.0385
	Oral/Throat Disorders				
'327.23'	Obstructive sleep apnea (adult)(pediatric)	1.05	0.92	1.2	0.4486
'780.53'	Hypersomnia with sleep apnea, unspecified	0.94	0.67	1.3	0.6861
'780.57'	Unspecified sleep apnea	0.89	0.67	1.18	0.4091
'787.20'	Dysphagia, unspecified	0.92	0.74	1.14	0.4373
'787.22'	Dysphagia, oropharyngeal phase	1.2	0.78	1.86	0.3971
	Sleep Disorders				
'327.42'	REM sleep behavior disorder	0.9	0.63	1.29	0.5660
'333.94'	Restless legs syndrome (RLS)	0.7	0.42	1.19	0.1769
	Speech				
'784.59'	Other speech disturbance	1.03	0.57	1.86	0.9274
'V57.3'	Care involving speech-language therapy	1.3	0.86	1.96	0.2007
	Urinary				
'596.51'	Hypertonicity of bladder	0.84	0.62	1.14	0.2528
'596.54'	Neurogenic bladder NOS	0.66	0.46	0.94	0.0205
'788.20'	Retention of urine, unspecified	0.48	0.36	0.62	< 0.0001

'788.31'	Urge incontinence	0.75	0.59	0.94	0.0125
	Other				
'458.0'	Orthostatic hypotension	0.66	0.48	0.91	0.0101
'458.9'	Hypotension, unspecified	0.72	0.55	0.95	0.0186
'564.00'	Constipation, unspecified	0.72	0.61	0.85	0.0001
'607.84'	Impotence of organic origin	1.09	0.86	1.37	0.4676
Complications					
	Cerebral, Brain				
'331.9'	Cerebral degeneration, unspecified	0.88	0.72	1.09	0.2361
'348.30'	Encephalopathy, unspecified	0.55	0.33	0.91	0.0175
	Infections				
'038.9'	Unspecified septicemia	0.58	0.35	0.95	0.0285
'482.9'	Bacterial pneumonia, unspecified	0.72	0.38	1.38	0.3189
'790.7'	Bacteremia	0.61	0.19	1.91	0.3865
'995.91'	Sepsis	0.53	0.31	0.89	0.0141
	Pressure Ulcers				
'707.00'	Pressure ulcer, unspecified site	0.61	0.28	1.36	0.2179
'707.03'	Pressure ulcer, lower back	0.73	0.38	1.38	0.323
'707.05'	Pressure ulcer, buttock	0.44	0.2	0.96	0.0357
	Weakness and Pain				
'338.29'	Other chronic pain	0.64	0.43	0.94	0.0213
'719.49'	Pain in joint, multiple sites	1.44	0.82	2.52	0.1952
'724.2'	Lumbago	1	0.88	1.14	0.9981
'724.5'	Backache, unspecified	0.94	0.77	1.15	0.5558
'728.2'	Muscular wasting and disuse atrophy, not elsewhere classified	0.49	0.22	1.09	0.076
'728.87'	Muscle weakness (generalized)	0.68	0.56	0.82	1.00E-04
'780.79'	Other malaise and fatigue	0.74	0.66	0.85	0.0001
'783.21'	Loss of weight	0.96	0.78	1.19	0.7209
'783.7'	Adult failure to thrive	0.46	0.21	1	0.0469
'799.3'	Debility, unspecified	0.74	0.55	1	0.0427
	Other				
'276.51'	Dehydration	0.77	0.59	1	0.0465
'728.85'	Spasm of muscle	1.07	0.65	1.76	0.7867

'780.2'	Syncope and collapse	0.68	0.56	0.83	0.0001
'780.52'	Insomnia, unspecified	0.88	0.64	1.22	0.4451
'782.3'	Edema	0.88	0.76	1.02	0.0832
'784.51'	Dysarthria	0.84	0.47	1.49	0.5367
'959.01'	Head injury, unspecified	0.7	0.59	0.83	< 0.0001

Table S1: Relative risk of ICD-9-CM diagnostic codes identified by neurologist review as being PD-related. Codes are organized by the major grouping (“motor”, “non-motor” and “complications”) and additionally within clinically relevant/organ system groupings. A total of 79 codes were identified as being PD-related and 42 had a statistically significant reduction in incidence in the AZ/DZ/TZ group relative to the tamsulosin group.

Label	Relative Risk	95% LB	95% UB	P-Value
Motor	0.77	0.70	0.84	< 0.0001
Walking, gait, coordination	0.75	0.68	0.83	< 0.0001
Falls	0.63	0.50	0.79	< 0.0001
Essential/Other Tremor	1.23	1.02	1.49	0.0260
Other	0.71	0.57	0.88	0.0012
Non-Motor	0.78	0.73	0.83	< 0.0001
Dementia	0.68	0.60	0.78	< 0.0001
Neuropsychiatric	0.78	0.67	0.91	0.0018
Oral/Throat Disorders	1.03	0.92	1.16	0.5490
Sleep Disorders	0.76	0.52	1.10	0.1392
Speech	1.16	0.82	1.64	0.3974
Urinary	0.58	0.48	0.69	< 0.0001
Other	0.75	0.66	0.85	< 0.0001
Complications	0.76	0.71	0.82	< 0.0001
Cerebral, Brain	0.68	0.51	0.91	0.0088
Infections	0.60	0.41	0.88	0.0069
Pressure Ulcers	0.57	0.34	0.94	0.0241
Weakness and Pain	0.78	0.71	0.86	< 0.0001
Other	0.80	0.72	0.88	< 0.0001

Table S2: Relative risk of clinically relevant/organ system clustering of expert identified PD-related ICD-9-CM diagnostic codes. A total of 16 sub-groups were identified and relative risk was statistically significantly reduced in the AZ/DZ/TZ group for 12 of those groups.

Table S3. Statistical analyses.

Figure		Test	Comparison	P value
Fig 1C		Mann-Whitney	Vehicle vs. TZ	0.0022
Fig 1D		Mann-Whitney	Vehicle vs. TZ	0.0260
Fig 1E		Kruskal-Wallis	Overall	<0.0001
		Dunn's	0 vs 0.1 ug/Kg TZ	
		Dunn's	0 vs 1 ug/Kg TZ	0.0004
		Dunn's	0 vs 10 ug/Kg TZ	0.0001
		Dunn's	0 vs 100 ug/Kg TZ	0.0300
		Dunn's	0 vs 1000 ug/Kg TZ	0.2779
Fig 1F		Kruskal-Wallis	Overall	0.0011
		Dwass-Steele-Critchlow-Fligner	Vehicle vs. MPTP	0.0644
		Dwass-Steele-Critchlow-Fligner	Vehicle vs. MPTP+TZ	0.0110
		Dwass-Steele-Critchlow-Fligner	MPTP vs. MPTP+TZ	0.0110
Fig 1G		Kruskal-Wallis	Overall	0.0054
		Dwass-Steele-Critchlow-Fligner	Vehicle vs. MPTP	0.0110
		Dwass-Steele-Critchlow-Fligner	Vehicle vs. MPTP+TZ	0.7977
		Dwass-Steele-Critchlow-Fligner	MPTP vs. MPTP+TZ	0.0281
Fig 2C	day 7	Mann-Whitney	Vehicle vs. TZ	0.0043
	day 14	Mann-Whitney	Vehicle vs. TZ	0.0022
Fig 2D	day 7	Mann-Whitney	Vehicle vs. TZ	0.0022
	day 14	Mann-Whitney	Vehicle vs. TZ	0.0022
Fig 2F	day 7	Mann-Whitney	Vehicle vs. TZ	0.0152
	day 14	Mann-Whitney	Vehicle vs. TZ	0.0022
Fig 2G	day 7	Mann-Whitney	Vehicle vs. TZ	0.0232
	day 14	Mann-Whitney	Vehicle vs. TZ	0.0187
Fig 2H	day 7	Mann-Whitney	Vehicle vs. TZ	0.0022
	day 14	Mann-Whitney	Vehicle vs. TZ	0.0022

Fig 2I	day 7	Mann-Whitney	Vehicle vs. TZ	0.1000
	day 14	Mann-Whitney	Vehicle vs. TZ	0.0043
Fig 2J	day 7	Mann-Whitney	Vehicle vs. TZ	0.0649
	day 14	Mann-Whitney	Vehicle vs. TZ	0.0022
Fig 2K	day 7	Mann-Whitney	Vehicle vs. TZ	0.0022
	day 14	Mann-Whitney	Vehicle vs. TZ	0.0260
Fig 3B	week 4	Mann-Whitney	Vehicle vs. TZ	0.0138
	week 5	Mann-Whitney	Vehicle vs. TZ	0.0003
	week 6	Mann-Whitney	Vehicle vs. TZ	0.0232
	week 7	Mann-Whitney	Vehicle vs. TZ	0.0022
Fig 3C	week 4	Kruskal-Wallis	Overall	0.0002
		Dwass-Steele-Critchlow-Fligner	Vehicle vs. 6-OHDA	0.0206
		Dwass-Steele-Critchlow-Fligner	Vehicle vs. TZ	0.9886
		Dwass-Steele-Critchlow-Fligner	Vehicle vs. 6-OHDA+TZ	0.0206
		Dwass-Steele-Critchlow-Fligner	6-OHDA vs. TZ	0.0206
		Dwass-Steele-Critchlow-Fligner	6-OHDA vs. 6-OHDA+TZ	0.0206
		Dwass-Steele-Critchlow-Fligner	TZ vs. 6-OHDA+TZ	0.2060
	week 5	Kruskal-Wallis	Overall	0.0002
		Dwass-Steele-Critchlow-Fligner	Vehicle vs. 6-OHDA	0.0206
		Dwass-Steele-Critchlow-Fligner	Vehicle vs. TZ	0.9951
		Dwass-Steele-Critchlow-Fligner	Vehicle vs. 6-OHDA+TZ	0.0206
		Dwass-Steele-Critchlow-Fligner	6-OHDA vs. TZ	0.0206
		Dwass-Steele-Critchlow-Fligner	6-OHDA vs. 6-OHDA+TZ	0.0206
		Dwass-Steele-Critchlow-Fligner	TZ vs. 6-OHDA+TZ	0.0206
	week 6	Kruskal-Wallis	Overall	0.0002
		Dwass-Steele-Critchlow-Fligner	Vehicle vs. 6-OHDA	0.0206
		Dwass-Steele-Critchlow-Fligner	Vehicle vs. TZ	0.9886
		Dwass-Steele-Critchlow-Fligner	Vehicle vs. 6-OHDA+TZ	0.0206
		Dwass-Steele-Critchlow-Fligner	6-OHDA vs. TZ	0.0206
		Dwass-Steele-Critchlow-Fligner	6-OHDA vs. 6-OHDA+TZ	0.0206
		Dwass-Steele-Critchlow-Fligner	TZ vs. 6-OHDA+TZ	0.0206
	week 7	Kruskal-Wallis	Overall	0.0002
		Dwass-Steele-Critchlow-Fligner	Vehicle vs. 6-OHDA	0.0206
		Dwass-Steele-Critchlow-Fligner	Vehicle vs. TZ	0.9886
		Dwass-Steele-Critchlow-Fligner	Vehicle vs. 6-OHDA+TZ	0.0206
		Dwass-Steele-Critchlow-Fligner	6-OHDA vs. TZ	0.0206

		Dwass-Steele-Critchlow-Fligner	6-OHDA vs. 6-OHDA+TZ	0.0206
		Dwass-Steele-Critchlow-Fligner	TZ vs. 6-OHDA+TZ	0.0206
Fig 3D		Kruskal-Wallis	Overall	0.0005
		Dwass-Steele-Critchlow-Fligner	Vehicle vs. 6-OHDA	0.0206
		Dwass-Steele-Critchlow-Fligner	Vehicle vs. TZ	0.9189
		Dwass-Steele-Critchlow-Fligner	Vehicle vs. 6-OHDA+TZ	0.0509
		Dwass-Steele-Critchlow-Fligner	6-OHDA vs. TZ	0.0206
		Dwass-Steele-Critchlow-Fligner	6-OHDA vs. 6-OHDA+TZ	0.0767
		Dwass-Steele-Critchlow-Fligner	TZ vs. 6-OHDA+TZ	0.0329
Fig 3E		Kruskal-Wallis	Overall	0.0009
		Dwass-Steele-Critchlow-Fligner	Vehicle vs. 6-OHDA	0.0206
		Dwass-Steele-Critchlow-Fligner	Vehicle vs. TZ	0.9635
		Dwass-Steele-Critchlow-Fligner	Vehicle vs. 6-OHDA+TZ	0.1121
		Dwass-Steele-Critchlow-Fligner	6-OHDA vs. TZ	0.0206
		Dwass-Steele-Critchlow-Fligner	6-OHDA vs. 6-OHDA+TZ	0.0329
		Dwass-Steele-Critchlow-Fligner	TZ vs. 6-OHDA+TZ	0.1329
Fig 3F	week 4	Mann-Whitney	Vehicle vs. TZ	<0.0001
	week 5	Mann-Whitney	Vehicle vs. TZ	<0.0001
	week 6	Mann-Whitney	Vehicle vs. TZ	0.0024
	week 7	Mann-Whitney	Vehicle vs. TZ	0.0410
Fig 3G	Left paw	Friedman	Overall	0.0042
		Dunn's	Vehicle vs 6-OHDA	0.0102
		Dunn's	Vehicle vs 6-OHDA+TZ	>0.9999
		Dunn's	6-OHDA vs 6-OHDA+TZ	0.0184
	Right paw	Friedman	Overall	0.0556
		Dunn's	Vehicle vs 6-OHDA	0.2669
		Dunn's	Vehicle vs 6-OHDA+TZ	>0.9999
		Dunn's	6-OHDA vs 6-OHDA+TZ	0.0700
	Both paws	Friedman	Overall	0.5896
		Dunn's	Vehicle vs 6-OHDA	>0.9999
		Dunn's	Vehicle vs 6-OHDA+TZ	>0.9999
		Dunn's	6-OHDA vs 6-OHDA+TZ	>0.9999

Fig 4B		Kruskal-Wallis	Overall	0.0015
		Dwass-Steele-Critchlow-Fligner	Vehicle vs rotenone	0.0110
		Dwass-Steele-Critchlow-Fligner	Vehicle vs rotenone+TZ	0.1326
		Dwass-Steele-Critchlow-Fligner	rotenone vs rotenone+TZ	0.0110
Fig 4C		ANOVA	Overall	<0.0001
		Tukey	Vehicle vs rotenone	<0.0001
		Tukey	Vehicle vs rotenone+1uM TZ	0.0007
		Tukey	rotenone vs rotenone+1uM TZ	0.0105
Fig 4D		Paired t-test	Control vs PGK1 RNAi	0.0006
Fig 4E		ANOVA	Overall	<0.0001
		Tukey	W^{1118} vs Pgk RNAi	0.8252
		Tukey	W^{1118} vs Pgk RNAi+rotenone	<0.0001
		Tukey	W^{1118} vs Pgk RNAi+rotenone+TZ	<0.0001
		Tukey	Pgk RNAi vs Pgk RNAi+rotenone	<0.0001
		Tukey	Pgk RNAi vs Pgk RNAi+rotenone+TZ	<0.0001
		Tukey	Pgk RNAi+rotenone vs Pgk RNAi+rotenone+TZ	0.9291
Fig 4F	Control	Unpaired t-test	Vehicle vs rotenone	0.0028
	TH>Pgk	Unpaired t-test	Vehicle vs rotenone	0.0350
	Appl>Pgk	Unpaired t-test	Vehicle vs rotenone	0.8205
	Actin>Pgk	Unpaired t-test	Vehicle vs rotenone	0.9725
	Mhc>Pgk	Unpaired t-test	Vehicle vs rotenone	0.0092
Fig 5A		Kruskal-Wallis	Overall	0.0004
		Dwass-Steele-Critchlow-Fligner	w^{1118} vs $PINK1^{5}$	0.0055
		Dwass-Steele-Critchlow-Fligner	w^{1118} vs $PINK1^{5}$+TZ	0.0058
		Dwass-Steele-Critchlow-Fligner	$PINK1^{5}$ vs $PINK1^{5}$+TZ	0.0102
Fig 5C		Kruskal-Wallis	Overall	0.0019
		Dwass-Steele-Critchlow-Fligner	w^{1118} vs $PINK1^{5}$	0.0245
		Dwass-Steele-Critchlow-Fligner	w^{1118} vs $PINK1^{5}$+TZ	0.0245
		Dwass-Steele-Critchlow-Fligner	$PINK1^{5}$ vs $PINK1^{5}$+TZ	0.0245

Fig 5D	ANOVA	Overall	0.0003
	Tukey	w^{1118} vs $PINK1^{5}$	0.0003
	Tukey	w^{1118} vs $PINK1^{5}$+TZ	0.0017
	Tukey	$PINK1^{5}$ vs $PINK1^{5}$+TZ	0.0910
Fig 5E	Kruskal-Wallis	Overall	0.0004
	Dwass-Steele-Critchlow-Fligner	w^{1118} vs $PINK1^{5}$	0.0047
	Dwass-Steele-Critchlow-Fligner	w^{1118} vs $PINK1^{5}$+TZ	0.0049
	Dwass-Steele-Critchlow-Fligner	$PINK1^{5}$ vs $PINK1^{5}$+TZ	0.0622
Fig 5F	Kruskal-Wallis	Overall	0.0007
	Dwass-Steele-Critchlow-Fligner	w^{1118} vs $LRRK^{ex1}$	0.0099
	Dwass-Steele-Critchlow-Fligner	w^{1118} vs $LRRK^{ex1}$+TZ	0.0100
	Dwass-Steele-Critchlow-Fligner	$LRRK^{ex1}$ vs $LRRK^{ex1}$+TZ	0.0260
Fig 5I	Kruskal-Wallis	Overall	0.0015
	Dwass-Steele-Critchlow-Fligner	WT vs mThy-hSCNA	0.0148
	Dwass-Steele-Critchlow-Fligner	WT vs mThy-hSCNA+TZ	0.0148
	Dwass-Steele-Critchlow-Fligner	mThy-hSCNA vs mThy-hSCNA+TZ	0.0245
Fig 5J	Kruskal-Wallis	Overall	0.0015
	Dwass-Steele-Critchlow-Fligner	WT vs mThy-hSCNA	0.0148
	Dwass-Steele-Critchlow-Fligner	WT vs mThy-hSCNA+TZ	0.0148
	Dwass-Steele-Critchlow-Fligner	mThy-hSCNA vs mThy-hSCNA+TZ	0.0245
Fig 5K	Kruskal-Wallis	Overall	0.0098
	Dwass-Steele-Critchlow-Fligner	WT vs mThy-hSCNA	0.0245
	Dwass-Steele-Critchlow-Fligner	WT vs mThy-hSCNA+TZ	0.1160
	Dwass-Steele-Critchlow-Fligner	mThy-hSCNA vs mThy-hSCNA+TZ	0.1778
Fig 6B	Mann-Whitney	Control vs Control+TZ	0.7000
	Mann-Whitney	$LRRK2^{G2019S}$ vs $LRRK2^{G2019S}$+TZ	0.0002
Fig 6C	Mann-Whitney	Control vs Control+TZ	0.0332
	Mann-Whitney	$LRRK2^{G2019S}$ vs $LRRK2^{G2019S}$+TZ	0.0068
Fig S1B	Mann-Whitney	SNC: Vehicle vs. TZ	0.0411
	Mann-Whitney	Cortex: Vehicle vs TZ	0.0022

Fig S1C		Mann-Whitney	SNC: Vehicle vs. TZ	0.0043
		Mann-Whitney	Cortex: Vehicle vs TZ	0.0022
Fig S1D		Kruskal-Wallis	Overall	<0.0001
		Dunn's	SNc: 0 vs 0.1 ug/Kg TZ	0.2119
		Dunn's	SNc: 0 vs 1 ug/Kg TZ	0.0011
		Dunn's	SNc: 0 vs 10 ug/Kg TZ	<0.0001
		Dunn's	SNc: 0 vs 100 ug/Kg TZ	0.0131
		Dunn's	SNc: 0 vs 1000 ug/Kg TZ	0.3239
		Kruskal-Wallis	Overall	<0.0001
		Dunn's	Cortex: 0 vs 0.1 ug/Kg TZ	0.6811
		Dunn's	Cortex: 0 vs 1 ug/Kg TZ	0.0037
		Dunn's	Cortex: 0 vs 10 ug/Kg TZ	<0.0001
		Dunn's	Cortex: 0 vs 100 ug/Kg TZ	0.0689
		Dunn's	Cortex: 0 vs 1000 ug/Kg TZ	0.0689
Fig S2B		Kruskal-Wallis	Overall	0.0006
		Dwass-Steele-Critchlow-Fligner	Vehicle vs. MPTP	0.0110
		Dwass-Steele-Critchlow-Fligner	Vehicle vs. MPTP+TZ	0.0178
		Dwass-Steele-Critchlow-Fligner	MPTP vs. MPTP+TZ	0.0110
Fig S2C		Kruskal-Wallis	Overall	0.0078
		Dwass-Steele-Critchlow-Fligner	Vehicle vs. MPTP	0.0281
		Dwass-Steele-Critchlow-Fligner	Vehicle vs. MPTP+TZ	0.7977
		Dwass-Steele-Critchlow-Fligner	MPTP vs. MPTP+TZ	0.0178
Fig S2D	Striatum 16S	ANOVA	Overall	<0.0001
		Tukey	Vehicle vs. MPTP	0.0002
		Tukey	Vehicle vs. MPTP+TZ	0.4628
		Tukey	MPTP vs. MPTP+TZ	<0.0001
	Striatum ND1	ANOVA	Overall	0.1047
		Tukey	Vehicle vs. MPTP	0.1761
		Tukey	Vehicle vs. MPTP+TZ	0.9470
		Tukey	MPTP vs. MPTP+TZ	0.1178

	SNc 16S	ANOVA	Overall	0.1273
		Tukey	Vehicle vs. MPTP	0.1115
		Tukey	Vehicle vs. MPTP+TZ	0.4327
		Tukey	MPTP vs. MPTP+TZ	0.5458
	SNc ND1	ANOVA	Overall	0.0320
		Tukey	Vehicle vs. MPTP	0.1174
		Tukey	Vehicle vs. MPTP+TZ	0.5343
		Tukey	MPTP vs. MPTP+TZ	0.0291
Fig S2E	Striatum	Kruskal-Wallis	Overall	0.0006
		Dwass-Steele-Critchlow-Fligner	Vehicle vs. MPTP	0.0110
		Dwass-Steele-Critchlow-Fligner	Vehicle vs. MPTP+TZ	0.0178
		Dwass-Steele-Critchlow-Fligner	MPTP vs. MPTP+TZ	0.0110
	SNc	Kruskal-Wallis	Overall	0.0051
		Dwass-Steele-Critchlow-Fligner	Vehicle vs. MPTP	0.0178
		Dwass-Steele-Critchlow-Fligner	Vehicle vs. MPTP+TZ	0.0644
		Dwass-Steele-Critchlow-Fligner	MPTP vs. MPTP+TZ	0.1326
Fig S2F	Striatum	Kruskal-Wallis	Overall	0.0028
		Dwass-Steele-Critchlow-Fligner	Vehicle vs. MPTP	0.0110
		Dwass-Steele-Critchlow-Fligner	Vehicle vs. MPTP+TZ	0.6017
		Dwass-Steele-Critchlow-Fligner	MPTP vs. MPTP+TZ	0.0110
	SNc	Kruskal-Wallis	Overall	0.0025
		Dwass-Steele-Critchlow-Fligner	Vehicle vs. MPTP	0.0110
		Dwass-Steele-Critchlow-Fligner	Vehicle vs. MPTP+TZ	0.0431
		Dwass-Steele-Critchlow-Fligner	MPTP vs. MPTP+TZ	0.0936
Fig S3A		Mann-Whitney	Vehicle vs. TZ	0.0043
Fig S3B		Mann-Whitney	Vehicle vs. TZ	0.0152
Fig S3C		Mann-Whitney	Vehicle vs. TZ	0.0043
Fig S3D		Kruskal-Wallis	Overall	0.0001
		Dwass-Steele-Critchlow-Fligner	Vehicle vs. TZ	0.0206
		Dwass-Steele-Critchlow-Fligner	Vehicle vs. MPP^+	0.0206
		Dwass-Steele-Critchlow-Fligner	Vehicle vs. MPP^++TZ	0.0509
		Dwass-Steele-Critchlow-Fligner	TZ vs. MPP^+	0.0206
		Dwass-Steele-Critchlow-Fligner	TZ vs. MPP^++TZ	0.0206
		Dwass-Steele-Critchlow-Fligner	MPP^+ vs MPP^++TZ	0.0206

Fig S3E		Kruskal-Wallis	Overall	0.0001
		Dwass-Steele-Critchlow-Fligner	Vehicle vs. TZ	0.1591
		Dwass-Steele-Critchlow-Fligner	Vehicle vs. MPP^+	0.0206
		Dwass-Steele-Critchlow-Fligner	Vehicle vs. MPP^++TZ	0.0206
		Dwass-Steele-Critchlow-Fligner	TZ vs. MPP^+	0.0206
		Dwass-Steele-Critchlow-Fligner	TZ vs. MPP^++TZ	0.0206
		Dwass-Steele-Critchlow-Fligner	MPP^+ vs MPP^++TZ	0.0206
Fig S3F		Unpaired t-test	Blood vs CSF	0.0030
Fig S4C	day 7	Mann-Whitney	Vehicle vs. TZ	0.0022
	day 14	Mann-Whitney	Vehicle vs. TZ	0.0043
Fig S4D	day 7	Mann-Whitney	Vehicle vs. TZ	0.0173
	day 14	Mann-Whitney	Vehicle vs. TZ	0.0152
Fig S4E	day 7	Mann-Whitney	Vehicle vs. TZ	0.0152
	day 14	Mann-Whitney	Vehicle vs. TZ	0.0411
Fig S4F	day 7	Mann-Whitney	Vehicle vs. TZ	0.0022
	day 14	Mann-Whitney	Vehicle vs. TZ	0.0260
Fig S4H		ANOVA	Overall	0.5337
Fig S4I		Mann-Whitney	Vehicle vs. TZ	0.0005
Fig S4J		Mann-Whitney	Vehicle vs. TZ	0.0407
Fig S5E	week 4	Kruskal-Wallis	Overall	0.0002
		Dwass-Steele-Critchlow-Fligner	Vehicle vs. 6-OHDA	0.0206
		Dwass-Steele-Critchlow-Fligner	Vehicle vs. TZ	0.9886
		Dwass-Steele-Critchlow-Fligner	Vehicle vs. 6-OHDA+TZ	0.0206
		Dwass-Steele-Critchlow-Fligner	6-OHDA vs. TZ	0.0206
		Dwass-Steele-Critchlow-Fligner	6-OHDA vs. 6-OHDA+TZ	0.0206
		Dwass-Steele-Critchlow-Fligner	TZ vs. 6-OHDA+TZ	0.0206
	week 5	Kruskal-Wallis	Overall	0.0002

		Dwass-Steele-Critchlow-Fligner	Vehicle vs. 6-OHDA	0.0206
		Dwass-Steele-Critchlow-Fligner	Vehicle vs. TZ	0.9635
		Dwass-Steele-Critchlow-Fligner	Vehicle vs. 6-OHDA+TZ	0.0203
		Dwass-Steele-Critchlow-Fligner	6-OHDA vs. TZ	0.0206
		Dwass-Steele-Critchlow-Fligner	6-OHDA vs. 6-OHDA+TZ	0.0203
		Dwass-Steele-Critchlow-Fligner	TZ vs. 6-OHDA+TZ	0.0203
	week 6	Kruskal-Wallis	Overall	0.0003
		Dwass-Steele-Critchlow-Fligner	Vehicle vs. 6-OHDA	0.0203
		Dwass-Steele-Critchlow-Fligner	Vehicle vs. TZ	0.8879
		Dwass-Steele-Critchlow-Fligner	Vehicle vs. 6-OHDA+TZ	0.0203
		Dwass-Steele-Critchlow-Fligner	6-OHDA vs. TZ	0.0206
		Dwass-Steele-Critchlow-Fligner	6-OHDA vs. 6-OHDA+TZ	0.0922
		Dwass-Steele-Critchlow-Fligner	TZ vs. 6-OHDA+TZ	0.0206
	week 7	Kruskal-Wallis	Overall	0.0002
		Dwass-Steele-Critchlow-Fligner	Vehicle vs. 6-OHDA	0.0203
		Dwass-Steele-Critchlow-Fligner	Vehicle vs. TZ	0.9985
		Dwass-Steele-Critchlow-Fligner	Vehicle vs. 6-OHDA+TZ	0.0200
		Dwass-Steele-Critchlow-Fligner	6-OHDA vs. TZ	0.0206
		Dwass-Steele-Critchlow-Fligner	6-OHDA vs. 6-OHDA+TZ	0.0203
		Dwass-Steele-Critchlow-Fligner	TZ vs. 6-OHDA+TZ	0.0203
Fig S5F		ANOVA	Overall	0.9937
Fig S5G	week 4	Mann-Whitney	Vehicle vs. TZ	0.0022
	week 5	Mann-Whitney	Vehicle vs. TZ	0.0649
	week 6	Mann-Whitney	Vehicle vs. TZ	0.0649
	week 7	Mann-Whitney	Vehicle vs. TZ	0.1797
Fig S5H	week 4	Mann-Whitney	Vehicle vs. TZ	0.0022
	week 5	Mann-Whitney	Vehicle vs. TZ	0.0130
	week 6	Mann-Whitney	Vehicle vs. TZ	0.0931
	week 7	Mann-Whitney	Vehicle vs. TZ	0.1797
Fig S6A		ANOVA	Overall	<0.0001
		Dunnet's	w^{1118} day 10 vs $PINK1^{5}$ day 1	0.6720
		Dunnet's	w^{1118} day 10 vs $PINK1^{5}$ day 5	0.0002

		Dunnet's	w^{1118} day 10 vs $PINK1^{5}$ day 10	<0.0001
Fig S6B		Kruskal-Wallis		0.0003
		Dwass-Steele-Critchlow-Fligner	w^{1118} vs $PINK1^{5}$	0.0020
		Dwass-Steele-Critchlow-Fligner	w^{1118} vs $PINK1^{5}$+TZ	0.0305
		Dwass-Steele-Critchlow-Fligner	$PINK1^{5}$ vs $PINK1^{5}$+TZ	0.0187
Fig S6C		Mann-Whitney	w^{1118} vs $PINK1^{5}$	0.0006
Fig S7A		Mann-Whitney	Vehicle vs. TZ	0.0317
Fig S7B		Mann-Whitney	Vehicle vs. TZ	0.2222
Fig S9A	OCR	Kruskal-Wallis	Overall	0.0094
		Dunn's	Vehicle vs TZ	0.0180
		Dunn's	Vehicle vs AZ	0.0066
		Dunn's	Vehicle vs DZ	0.0180
	ECAR	Kruskal-Wallis	Overall	0.0124
		Dunn's	Vehicle vs TZ	0.0159
		Dunn's	Vehicle vs AZ	0.0159
		Dunn's	Vehicle vs DZ	0.0112
Fig S9B		Kruskal-Wallis	Overall	0.0015
		Dunn's	Vehicle vs urapadil	0.9999
		Dunn's	Vehicle vs tamsulosin	0.9999
		Dunn's	Vehicle vs TZ	0.0256
		Dunn's	Vehicle vs DZ	0.4457
		Dunn's	Vehicle vs AZ	0.0069

METHODS

Title: Enhancing Glycolysis Attenuates Parkinson's Disease in Models and Clinical Databases

Chemicals

1-Methyl-4-phenyl-1,2,3,6-tetrahydropyridine (MPTP), 6-Hydroxydopamine hydrobromide (6-OHDA), 1-methyl-4-phenylpyridinium (MPP^+), rotenone, apomorphine hydrochloride, tamsulosin hydrochloride, urapidil hydrochloride, phenylephrine hydrochloride, terazosin hydrochloride, doxazosin mesylate, alfuzosin hydrochloride, and prazosin hydrochloride were purchased from Sigma-Aldrich (St. Louis, MO, USA). The In Situ Cell Death Detection Kit was purchased from Roche Diagnostics (USA). The 3, 3-diaminobenzidine (DAB) kit was purchased from Beijing ComWin Biotech Co. Ltd. (Beijing, China). The EnzyChrom Pyruvate Assay Kit was purchased from BioAssay Systems (Hayward, CA, USA). The ATP assay kit was purchased from Promega Biotech (Beijing, China). The BCA Protein Assay Kit was purchased from Vigorous Biotechnology Beijing (Beijing, China). The Citrate Synthase (CS) Assay Kit was purchased from Nanjing Jiancheng Bioengineering Institute (Nanjing, China). The Nissl staining kit was purchased from Beyotime Biotech. (Beijing, China).

Antibodies

The antibodies used in immunohistochemistry and immunofluorescence were as follows: rabbit anti-tyrosine hydroxylase (1:2000, AB152, Millipore), goat anti-rabbit secondary antibody (1:200, BE0101, EasyBio Technology Co., Ltd.), and chicken anti-GFP (1:500, ab13970, Abcam). The antibodies used in iPSCs were mouse anti-human α-synuclein (610787, BD Biosciences, Madrid, Spain), rabbit anti-TH (sc-14007, Santa Cruz Biotechnology, Madrid), and mouse anti-TUJ1 (801202, Biolegend). The antibodies used in western blot were rabbit anti-TH (1:1000, AB152, Millipore), mouse anti-Pgk1/2 (1:200, sc-48342, Santa), mouse anti-human α-synuclein (1:500, 610787, BD Biosciences), rabbit anti-VDAC (1:1000, 8674, Cell Signaling), rabbit anti-PHB1 (1:1000, 8674, Cell Signaling) and mouse anti-β-actin (1:2000, HC201, TransGen Biotech).

Cell culture and hypoxia induction

The human BE(2)-M17 neuroblastoma cells were purchased from National Experimental Cell Resource Sharing Service Platform (Beijing, China). Cells were cultured in DMEM (Dulbecco's modified Eagle's medium) (Gibco), supplemented with 10% fetal bovine serum (Gibco) and 1% penicillin-streptomycin (Gibco), at 37 °C with 5% CO_2 and 95% air atmosphere in a humidified incubator (Thermo Scientific). Cells were incubated with mild hypoxia for 12 hr before study. Cells were cultured in a sealed chamber (Stemcell Technologies Vancouver, Canada) that was flushed with a humidified gas mixture composed of 5% O_2, 5% carbon dioxide (CO_2), and 90% nitrogen(N_2) for 12 hr. Three hours before harvest, the cells were switched to 5% CO_2 and 95% O_2 (1, 2). TZ (10 μM) or vehicle was added to the medium 15 hr before harvest. Assays of ATP, pyruvate, and citrate synthase activities (CS) were performed according to the manufacturer's instructions.

Animal maintenance

Male C57BL/6J mice (7 weeks old) and male Sprague-Dawley (SD) rats (200-220 g) were purchased from the Vital River Laboratory Animal Technology (Beijing, China). Animals were

housed under a 12 hr light/dark cycle with free access for food and water. All experiments using mice and rats were approved by the Institutional Animal Care and Use Committee, Peking University, Beijing (Approval NO: LSC-Liul-1 and LSC-Liul-2).

SNCA transgenic mice

SNCA transgenic mice(*mThy1-hSNCA*) were purchased from the Jackson Laboratory (017682, line15). *mThy1-hSNCA* express the human α-synuclein gene under the direction of the mouse thymus cell antigen 1 promoter (3). Mice were treated with TZ (0.03 mg/kg, oral) or vehicle from 3 months old and sacrificed at 15 months old. Behavioral tests were carried out during the TZ treatment period.

MPTP mouse model

After one week housing to adopt to the new environment, mice were randomly divided into six groups including the control group (saline injection) and the TZ group (0.1 μg/kg, 1 μg/kg,10 μg/kg, 100 μg/kg and 1000 μg/kg). MPTP was injected (i.p.) on one day at 20 mg/kg for four times at 2-hour intervals, as previously described (4). Beginning one week later, mice received a saline or TZ injection once a day. At the end of the drug or saline treatment, behavioral tests including rotarod test and pole test were carried out before the animals were sacrificed. As for the other drug tests (urapidil, tamsulosin, doxazosin, alfuzosin and prazosin), the experimental design was the same as for TZ.

Unilateral 6-OHDA lesion in rats

For the 6-OHDA model in rats, pentobarbital sodium (80 mg/kg) was used as anesthesia by i.p. injection. Then, the rats were fixed in a stereotaxic frame (Benchmark, myNeuroLab, S-072607). 6-OHDA was dissolved in 0.2 % ascorbic acid saline solution at 2.5 μg/μl. Unilateral injection of 6-OHDA was performed according to the stereotaxic atlas of rat (5). 6-OHDA was injected into two sites in the right striatum, with 10 μg for each site (coordinates with respects to bregma: AP, +0.8 mm; ML, +2.7 mm; DV, -5.2 mm; and AP, +0.8 mm; ML, +2.7 mm; DV, -4.5 mm) at a rate of 1 μl/min. using a 10-μl Hamilton syringe (6). The same amount of saline was injected the same way as a control. After the injection, the needle was left at the last site for another 5 min. before slow retraction. After the surgery, rats were placed on a warm electric blanket for recovery. Two weeks, three weeks, four weeks or five weeks later, apomorphine-induced rotational behavior was assessed to select the rats that had been successfully targeted. They were then randomly divided into two groups: saline treatment group and TZ treatment group (70 μg/kg i.p.). Based on the most effective doses of TZ at10 and 100 μg/kg in mice, we selected TZ at 70 μg/kg in rats. Sham-operated animals received saline in the same way. All these three groups were treated with saline or TZ for two weeks followed by locomotor activity assessment. After behavior testing, animals were sacrificed.

Two weeks after stereotaxic surgery, 6-OHDA-treated rats were given 0.5 mg/kg apomorphine (i.p.) (7). Then, the rats were placed in a transparent cylinder (diameter 30 cm, height 35 cm). Five min. later, contralateral rotation behavior was measured for 30 min. and recorded with a camera. The rats with a rotation rate over 7 turns/min. were selected for further studies (8).

Rotarod test

The rotarod test was carried out using an automated rotarod (E103, UGO BASILE). At a fixed speed of 15 revolutions per minute (rpm), mice were pre-trained for two consecutive days until they were able to remain on the rod for more than 60 seconds. On the 7th day and the 14th day after MPTP injection, mice were tested on the rotating rod at an acceleration mode (2-45 rpm). The latency to fall was recorded for a maximum recording time of 600 seconds. The behavior was monitored by a video camera.

Pole test in mice

This test was carried out by leaving a pole in the cage where the mice were housed. The pole test was performed on the 14th day after MPTP injection as previously described (9). The mouse was placed in a head-upward position on top of a vertical pole (diameter 8 mm, height 55 cm) with a ball (diameter 2.5 cm) on the head of the pole. The pole was wrapped with the nylon gauze to prevent the mouse from slipping down. Each mouse was trained twice before testing. The time that the mouse took to turn his head from upward to downward (Time: Turn) and the time the mouse took to reach the floor with his forepaws (Time: Locomotion Activity) were recorded. Each mouse was tested three times with 5 min. intervals, and the average time was quantified.

Cylinder test in rats

Forelimb movement coordination of rats was analyzed by the cylinder test as previously described (10). The rats were individually placed in a transparent cylinder (diameter 30 cm, height 35 cm). After 5 min. adaptation, their wall-contact with left, right or both fore-paws was counted until the total number of wall-contacts was 20. Then the percentage of left, right or both fore-paws touching were analyzed.

Immunohistochemistry and immunofluorescence

After anesthesia with pentobarbital sodium (80 mg/kg), animals were perfused with 0.9% saline followed by 4% ice-cold paraformaldehyde (PFA) in 0.1 M phosphate buffer (PBS, pH 7.4) as previously described (11). Brains were removed, post-fixed in PFA overnight, and transferred into 10%, 20% and 30% sucrose until brains successively sank to the bottom. Brains were cut into 30 μm thick coronal slices (in six series), free-floating sections were rinsed in PBS for three times, and quenched in 3% H_2O_2 for 10 min. Sections were pre-incubated in 2% BSA/0.3% triton x-100 in PBS (0.3% PBST) for one hour at room temperature, followed by incubation with primary antibody in the blocking solution overnight. To detect DA neuron cell bodies in the SNc and their fibers in the striatum, the rabbit anti-tyrosine hydroxylase (1:2000, AB152, Millipore) antibody was used. After three 10 min. washes with 0.3% PBST, brain sections were incubated with corresponding biotinylated secondary antibody (1:200, BE0101, EasyBio Technology Co., Ltd.), and subsequently incubated with avidin-biotin-peroxidase complex for one hour at room temperature. Then, the brain sections were treated with 3, 3′-diaminobenzidine and 0.01% H_2O_2 for 1-5 min. After dehydration in gradient alcohol and clearing in xylene, the brain slices were mounted on lysine pre-treated glass slides and cover-slipped in DPX (DPX mountant for histology). The brain slices were imaged under a stereoscope, and TH neurons and their fibers were analyzed using Stereo Investigator software (version 8) and Image-pro Plus 6.0, respectively. For immunofluorescence of the animal brain slices, the experimental procedures were similar to the immunohistochemistry protocol.

For immunofluorescence of iPSC-derived cells, cells were fixed with 4% paraformaldehyde (PFA) in PBS for 20 min. and blocked in 0.3% Triton X-100 (Sigma-Aldrich, Madrid, Spain) with 3% donkey serum for 2 hr, followed by incubation with primary antibodies 4 °C overnight and secondary antibodies at room temperature for 2 hr. In the case of α-synuclein staining, Triton X-100 was kept at 0.01% for the blocking and antibody incubation steps. Images were acquired using a Leica SP5 confocal microscope. We also performed a Sholl analysis, a widely used method to quantify the complexity of dendritic arbours. A Sholl profile is obtained by plotting the number of dendrite intersections against the radial distance from the soma center (12).

Western blot analysis

For protein detection, corresponding brain regions were harvested immediately after animals were euthanized and stored at -80 °C before protein extraction. RIPA buffer (Beyotime, Beijing, China) containing a cocktail of protease inhibitors (Roche, Mannheim, Germany) and PMSF (Sigma) were used for protein extraction according to a standard protocol (13). After disruption on ice for 30 min., the lysates were ultrasonicated and then centrifuged at 12,000 rpm for 15 min., and supernatants were harvested. Samples were separated on 12% SDS-polyacrylamide gels followed by transfer to PVDF membranes (Millipore, MA, USA). Membranes were blocked with 5% nonfat milk for one hour at room temperature and incubated with the primary antibody overnight at 4 °C. Membranes were washed 3 times for 10 min. with 0.1% Tween-20/PBS and then incubated with an IRDye 700 or 800-labeled secondary antibody (1:10000), and scanned with an Odyssey infrared imaging system (LI-COR instrument, Lincoln, NE, USA). The target protein levels were normalized to β-actin levels. The results were analyzed using the ImageJ2X software.

Striatal DA content detection

A high-performance liquid chromatography with electrochemical detector (HPLC-ECD) was used to detect the dopamine content as previously reported (14). Each animal tissue was accurately weighed and homogenized in 200 μl ice-chilled 0.1 M perchloric acid. The homogenate was centrifuged at 12,000 rpm for 20 min. at 4 °C, 160 μl of supernatant was collected and mixed with 80 μl ice-chilled solution B (20 mM potassium citrate, 300 mM dipotassium hydrogen phosphate, and 2 mM disodium ethylenediaminetetraacetate (EDTA-2Na), then centrifuged again and the supernatant was injected in HPLC for determination of catecholamines. Dopamine, DOPAC, and HVA content were reported as μg per mg wet tissue and normalized to the control group.

Assay of TZ in rat blood and CSF

HPLC-ECD was used to detect the TZ content in rat blood and cerebral spinal fluid (CSF). Rats were given 30 mg/kg TZ (i.p.), and blood and CSF samples were collected 20 min. after drug administration following a previous protocol (15). CSF was immediately preserved at -80 °C, while blood was equilibrated for 20 min. at room temperature and then centrifuged again for 15 min. at 4500 rpm, the supernatant was collected and stored at -80 °C. Blood and CSF samples were filtered using a 0.22 μm filter and 50 μl was used for detection. Standard curves were prepared with known amounts of TZ in double distilled water, yielding concentrations of 0, 1, 10 and 50 μg/ml. The content of TZ in CSF was divided by the TZ content in blood.

Mitochondrial DNA content

Relative mitochondria content can be estimated by the 16s *rRNA* and *ND1* (NADH dehydrogenase 1, a mitochondrial protein) (16). Mitochondrial DNA (mtDNA) was extracted from mouse brain tissues. After a rinse in PBS, tissues were placed in an ice-cold 1.5-ml microcentrifuge tube. 600 µl of lysis buffer (RIPA) was added to the tube, followed by 0.2 mg/ml proteinase K, to degrade the proteins present in the tissue sample. Then, samples were incubated at 55 °C for 3 hr. 100 µg/ml RNase A was added to degrade the RNA, incubated at 37 °C for 30 min. 250 µl of 7.5 M ammonium acetate and 600 µl of isopropanol were added, and mixed well. Samples were centrifuged for 10 min. at 15,000 x g at 4 °C, and the supernatant was removed. Pellets were washed with 500 µl 70% ethanol and dried for 10 min. Then the pellets were resuspended in 100 µl of TE buffer. The concentration of mtDNA was measured using a NanoDrop spectrophotometer, and a final concentration of 10 ng DNA/µl was used for qPCR. Primers are as follows:

16S rRNA forward and reverse primers:
F: 5'-CCGCAAGGGAAAGATGAAAGAC-3'
R: 5'-TCGTTTGGTTTCGGGGTTTC-3'

ND1 forward and reverse primers:
F: 5'-CTAGCAGAAACAAACCGGGC-3'
R: 5'-CCGGCTGCGTATTCTACGTT-3'

β-globin forward and reverse primers:
F: 5'- GAAGCGATTCTAGGGAGCAG-3'
R: 5'-GGAGCAGCGATTCTGAGTAGA-3'

***Drosophila* stock and rotenone toxicity assay**

The flies used in this study included w^{1118}, $PINK1^{5}$, $LRRK^{exl}$, *TH-Gal4, Appl-Gal4, Mhc-Gal4* and *Actin-Gal4* purchased from Bloomington Fly Stock Center and *Pgk RNAi* (Tsinghua TRiP RNAi stock, THU0568) purchased from Tsinghua TRiP RNAi stock. The *UAS-Pgk* transgene was generated by P-element insertion under the w^{1118} background by our laboratory. For all experiments, the flies were maintained in an incubator set with 25 °C and 60% humidity under a 12 hr light/dark cycle.

For the rotenone assay, 20 flies at 1-3 days old were collected and placed in each vial; for each experimental condition, 10 vials were tested. Rotenone (125 µM and 250 µM) were mixed in cornmeal fly food. The vial was replaced with a new vial every two days for a week. To assess behavioral performance, the flies were transferred into a transparent tube (height, 40 cm; diameter, 1.5 cm). Then, these flies were gently tapped to the bottom of the tube. Flies climbing past the 25 cm mark in 20 sec. were recorded as normal motor behavior (17).

$PINK1^{5}$ male flies were treated with TZ at 0 µM, 0.1 µM, 1 µM and 10 µM for 10 days from the 1st day after eclosion or TZ at 1 µM for 7 days from the 3rd day after eclosion. Wing defects were recorded every day or just at the end of TZ treatment depending on the experimental design. For TH neurons immunostaining and western blots, TZ was given to the adult flies after eclosion. After 18-20 days, fly heads were harvested. The PPL1 cluster of TH neurons were immunostained and counted.

LRRK^{exl} male flies were treated with TZ (1 μM) for 10 days after eclosion. The wing defects were recorded after 10 days of treatment.

Glycolysis and mitochondrial stress measured by XF^{e}-24 Seahorse assays

A Seahorse XF^{e} analyzer (XF^{e}-24, Seahorse Bioscience, Billerica, MA, USA) was used to measure the oxygen consumption rate (OCR) and the extracellular acidification rate (ECAR) as previously described (18). The M17 cells and iPS cells were seeded in XF^{e} 24-well plates (Seahorse Bioscience), while the plates used for iPS cells were poly-D-lysine pre-coated. Assay medium was prepared by supplementing Seahorse XF^{e}BaseMedium minimal DMEM (Seahorse Bioscience) with 2 mM L-glutamine for a Glycolysis Stress Test assay or 2 mM L-glutamine, 1 mM pyruvate and 10 mM glucose for a Mito Stress Test assay (Sigma). pH was adjusted to 7.4 at 37 °C. Probes (Seahorse Bioscience) were hydrated in the calibrant (Seahorse Bioscience) in a non-CO_2 incubator at 37 °C overnight. Cells were washed twice with assay medium and kept in a non-CO_2 incubator at 37 °C for 1 hr before analysis. Glucose, oligomycin and 2-deoxy-glucose (2-DG) were pre-loaded in the probe plate for Glycolysis Stress Test, while oligomycin, FCCP and a mixture of rotenone and antimycin A were used for Mito Stress Test.

ATP assay, citrate synthase activity, LDH assay and pyruvate level detection

Citrate synthase (CS) activity, LDH assay and pyruvate level were detected using commercial kits according to the manufacturer's directions. ATP content in animal tissues and M17 cells were detected with the ATP assay kit following the manufacturer's directions. ATP production by iPSCs was measured with the ATP Determination Kit (A22066, Molecular Probes) following the manufacturer's directions. 24 hr after plating, iPSC-derived neural progenitors were treated with 10 μM TZ for 24 hr. Cells were then washed with dPBS and detached with EDTA (AM9260G, Thermo Scientific) for counting. After washing them with ice-cold PBS, cells were centrifuged, and the supernatant was discarded. ATP buffer (100 nM Tris-HCL pH 7.75, 4 mM EDTA) was added. Cells were then flash frozen in liquid nitrogen, followed by a 3-min. boil, and 5 min. on ice. Cells were centrifuged at 4 ºC for 5 min. at 13,000 rpm. The supernatant was used with the ATP determination kit. Each reaction contained 1.25 μg/ml of firefly luciferase, 50 μM D-luciferin and 1 mM DTT in 1 X Reaction Buffer. After 15 min. incubation, luminescence was measured and the production of ATP per cell calculated.

Nissl staining

The brain slices of the striatum region were harvested for Nissl staining according to the protocol described above. Coronal slices (in six series) were mounted on lysine pre-treated glass slides, and dehydrated in gradient alcohol, cleared in xylene, cover-slipped in DPX followed by Nissl staining for 30 min. at room temperature. For neuron counting, six fields were randomly selected in one slice and six slices were used for each brain, three animals were counted for each group.

TUNEL assay

Mice and rat brain coronal slices (in six series) were collected for TUNEL assay, which was performed according to the manufacturer's protocol (Promega). Brain slices were fixed in 4% PFA for 15 min. at 15-25 °C, washed 3 times with PBS. Sections were incubated in permeabilization solution (0.3% triton x-100 in PBS) for 15 min. at 15-25 °C. Then, slices were treated with proteinase K (10 μg/ml) for 10 min. at 56 °C, followed by fixed in 4% PFA for 15

min. at 15-25 °C, and rinsed in PBS three times. TUNEL reaction buffer was added and incubated for 2 hr at 37 °C in a humidified atmosphere in the dark. After rinsing in PBS three times, samples were analyzed in a drop of PBS under a fluorescence microscope using an excitation wavelength in the range of 450-500 nm and detection in the range of 515-565 nm.

TUNEL/TH co-staining assay

Following immunohistochemistry, TUNEL was detected with the In Situ Cell Death Detection Kit (Roche Diagnostics, USA). Mouse brain slices were incubated with TUNEL reaction buffer for 2 hr at 37 °C. After rinsing with PBS 3 times, the samples were analyzed under a confocal microscope (Leica SP8, Germany).

RNA extraction and qRT-PCR

Flies of *actin>Pgk RNAi* and *actin>attp2* (as a control) were harvested, and total RNA was extracted using Trizol reagent according to the manufacturer's instructions (Invitrogen Life Technologies, CA, USA). Two μg RNA were reverse transcribed using the RevertAid First Strand cDNA Synthesis kit according to the manufacturer's protocol (Thermo Scientific). Real-time PCR analysis was performed followed the standard protocol from Applied Biosystems (7500 real-time PCR system, ABI Inc.). Actin was used as a reference for total RNA quantity. Primers are as follows:

Pgk forward and reverse primers:

F: 5'-ATCAAGTTGGCCCTTTCCAA-3'

R: 5'-CGACCCAAGTGGGACATCA-3'

Actin forward and reverse primers:

F: 5'- CGGCATCCACGAGACCACATAC-3'

R: 5'-TGATCTTGATCTTCATGGTTGAGGGA-3'

Cell culture experiments with iPSC cell lines derived from human patients

All procedures adhered to Spanish and EU guidelines and regulations for research involving the use of human pluripotent cell lines. The human iPSC lines used in our studies were generated following procedures approved by the Commission on Guarantees concerning the Donation and Use of Human Tissues and Cells of the Carlos III Health Institute, Madrid, Spain.

The human iPSC lines SP11 (from control), and SP12 and SP13 (from patients with familial PD carrying the $LRRK2^{G2019S}$ mutation) have been previously described (19). iPSC culture and differentiation toward midbrain DA neurons was carried out as described (20), following procedures approved by the Spanish competent authorities (Commission on Guarantees concerning the Donation and Use of Human Tissues and Cells of the Carlos III Health Institute). Briefly, iPSC were cultured on Matrigel (Corning Limited, Life Sciences, UK) and maintained in hESC medium, consisting of KO-DMEM supplemented with 20% KO-Serum Replacement, 2 mM Glutamax, 50 μM 2-mercaptoethanol (all from Invitrogen, Thermo Fisher Scientific, Madrid, Spain), non-essential amino acids (Cambrex, Nottingham, UK), and 10 ng/ml bFGF (Peprotech, London, UK). Medium was preconditioned overnight by irradiated mouse embryonic fibroblast and iPSC were cultured at 37 °C, 5% CO_2. For midbrain DA neuron differentiation, iPSC were disaggregated with Accutase and embryoid bodies (EB) generated using forced aggregation in V-shaped 96-well plates. Two days later, EBs were patterned as ventral midbrain by culturing them in suspension for 10 days in N2B27 supplemented with 100 ng/ml SHH, 100

ng/ml FGF8, and 10 ng/ml FGF2 (all from Peprotech, London, UK). Then, for α-synuclein and neurite analysis, differentiation to midbrain DA neurons was performed on the top of PA6 murine stromal cells for 3 weeks (PMID: 21877920). TH positive neurons in normal control was ~70%, and ~55% in subject 12 and 45% in subject 13 with *LRRK*^{G2019S} mutations. To analyze α-synuclein levels, neuronal cultures were gently trypsinized and re-plated on Matrigel-coated slides. One day and three days after plating, DA neurons were treated for 24 hr with 10 μM TZ, after which cells were fixed and analyzed.

Immunofluorescence analysis of iPSC-derived cells

iPSC-derived cells were fixed with 4% paraformaldehyde (PFA) in Tris-buffered saline (TBS) for 20 min. and blocked in 0.3% Triton X-100 (Sigma-Aldrich, Madrid, Spain) with 3% donkey serum for 2 hr. In the case of α-synuclein staining, Triton X-100 was kept at 0.01% for the blocking and antibody incubation steps. The following primary antibodies were used: mouse anti-α-synuclein (610787, BD Biosciences, Madrid, Spain), rabbit anti-TH (sc-14007, Santa Cruz Biotechnology, Madrid), and mouse anti-TUJ1 (801202, Biolegend). Images were acquired using a Leica SP5 confocal microscope.

Analysis of the Parkinson's Progression Markers Initiative (PPMI) database

We analyzed data from the PPMI database (21) for patients taking TZ alone, TZ/DZ/AZ, or tamsulosin. We tested if these drugs influenced the rate of motor progression as measured by part III of the Movement Disorder Society's Unified Parkinson's Disease Rating Scale (MDSUPDRS), which is a metric of motor disability in Parkinson's disease (22). For this analysis, only participants who were using TZ/DZ/AZ or tamsulosin at their baseline PPMI visit were included in the drug groups. PPMI protocol dictates that the fourth visit should occur approximately one year after the baseline visit; accordingly, any visit that occurred between the baseline visit and the fourth PPMI visit were included. Participants also had to have more than one visit to be included. Of the 13 participants in the TZ/DZ/AZ group, 11 were taking the medication-of-interest without breaks until their fourth visit. One participant was taking DZ at the time of their baseline visit, but discontinued within 30 days of their baseline visit. That participant was only considered to be using DZ during their first and second visits. Another participant was using AZ at their baseline visit and for approximately 5 months after that. This participant was considered to be taking AZ during their first and second visits. If these two participants were excluded from the analysis and only participants who were taking the medication-of-interest without breaks in therapy were included, the results change only marginally. The TZ/DZ/AZ group (n=11) has a slope of change of 0.02 ± 0.21 compared to 0.53 ± 0.05 in the control group (n=269, p=0.015). Only male participants were included as all patients taking TZ/DZ/AZ and tamsulosin were males. The indication for TZ/DZ/AZ and tamsulosin in all patients was benign prostatic hyperplasia or undefined urological problems. The characteristics of the patients are shown in Table 1.

Only MDS-UPDRS readings that were obtained when the participants were not yet taking a PD medication or were in the practically defined OFF state (at least 6 hours after the last dose of levodopa or any other anti-PD medication) were utilized for this analysis. We employed linear mixed effect regression (LMER) analyses to evaluate any differences in the slopes of the relative UPDRS scores between patients who were taking TZ, TZ/DZ/AZ, or tamsulosin compared to those who were not taking TZ/DZ/AZ. An unadjusted model was initially constructed that

included the MDS-UPDRS Part 3 score as the dependent variable and the duration * medication group interaction term as the independent variable. The model also allowed random intercepts per subject as well as differing slopes of time for each subject. In this unadjusted model, the monthly increase in the MDS-UPDRS Part 3 score in the control group was 0.31 ± 0.04 compared to a monthly decrease in MDS-UPDRS Part 3 of -0.21 ± 0.21 in the TZ/DZ/AZ group (p=0.013). We then constructed a similar model that was aimed to include covariates that may predict progression of the MDS-UPDRS Part 3 score over time. This model included age at baseline, age of symptom onset, use of PD medications at each visit, baseline MDS-UPDRS Part 3 score, and baseline Hoehn & Yahr score. In this adjusted model, the monthly increase in the MDS-UPDRS Part 3 score in the control group was 0.54 ± 0.05 compared to a monthly increase in MDS-UPDRS Part 3 of 0.04 ± 0.22 in the TZ/DZ/AZ group (p=0.022). Maximum likelihood methods were used to test differences in the intercepts and the slopes between groups. R was utilized for all analyses.

Analysis of the IBM Watson/Truven database

Cohort Identification

We identified male enrollees in the Truven Health Marketscan Commercial Claims and Encounters and Medicare Supplemental databases that had at least one outpatient diagnosis of Parkinson's disease (ICD-9 332.0, ICD-10 G20) between 2011 and 2016 and who were prescribed terazosin, doxazosin, or alfuzosin (TZ/DZ/AZ) or tamsulosin (control). Analysis was restricted to the initial period of uninterrupted time when an enrollee was plausibly taking one of the 4 drugs. Table 2 shows the numbers of enrollees, the person years of drug exposure, the age, and the average drug dosage.

ICD-9 to ICD-10 Translation

The ICD-9 to ICD-10 changeover happened on 2015-10-01. Approximately 25% of the diagnoses codes in our data are from ICD-10 while the rest are ICD-9 codes. Due to the relatively recent introduction of ICD-10, little work has previously been done using ICD-10 codes relative to the ICD-9 standard. To that end, we started by using only ICD-9 codes and then used the Centers for Medicare and Medicaid Services (CMS) ICD-9 to ICD-10 crosswalk as provided by the National Bureau of Economic Research. Recent publications have shown that the translations provided by this file are generally complete and reasonable translations, at least in the domain of cardiovascular outcomes (23).

Identifying Codes in PD Patients and PD-Related Codes

We identified the top 500 most commonly occurring ICD-9 codes among the cohort, regardless of whether or not enrollees were taking one of the drugs of interest (TZ/DZ/AZ and tamsulosin at the time). This comprised a set of common diagnostic codes that we used to search for differences in relative incidence. Days on which enrollees had the relevant diagnosis code were identified by matching the ICD-9 diagnosis code directly (2011-01-01 to 2015-09-31) or matching the crosswalked ICD-10 diagnosis code (2015-10-01 to 2016-12-31). Of the 500 considered codes, 497 occurred at least 50 times in the tamsulosin group and at least 50 times in the TZ/DZ/AZ group during the study period and were therefore included in the model.

The most frequent 497 ICD-9 codes were also reviewed by two neurologists whose clinical practice focuses on PD. Without knowledge of results, they labeled each code as either

potentially PD-related or unrelated to PD. A total of 80 codes were identified as PD-related. Because code 332.0 (Paralysis agitans) was used to identify patients with PD, we excluded that code from further analysis. That left us with a group of 79 PD-related codes. Those codes were further grouped as being motor, non-motor, or complications. The PD-related ICD-9 codes and their associated labels are listed in Table S1.

Defining Medication Days

We were interested in defining days when the enrollee had the medication and was plausibly taking the medication. We started by considering the proportion of days covered (PDC) measure of adherence. The PDC is simply the ratio of the number of days supplied provided in a dispensing event and the number of days until the next dispensing event for that medication (24, 25). A threshold of 80% is commonly considered "adherent to therapy" for medications used to manage diabetes and cardiovascular disease and is the threshold we selected here (26). A PDC of 80% corresponds to a refill occurring no more days later than 125% of the days supplied. For example, if a filled prescription (fill) had a 30 day supply, in order to have a PDC of at least 80% we would require a refill within 37.5 days (30 / 37.5 = 0.80). We identified each dispensing event and coded the following 125% of days supplied days as "taking the medication." After constructing this exposure variable for each fill, we constructed a variable for each person-day that took the value 1 if it was within 125% days supplied of any fill and 0 otherwise.

For each enrollee, we only used data from the first observed medication period. We chose not to include data from periods after the medication was potentially stopped and later restarted because the reason for changes in medication would be unknown and potentially could introduce confounding. We defined the first medication period to be all fills after the first fill such that there was no interval between fills longer than (125% of days supplied) + 90 days. We discarded any data after the first interval longer than this threshold between fills.

Analysis of the Codes

The effect of TZ/DZ/AZ *vs*. tamsulosin was estimated using a generalized linear model (GLM) with a quasi-Poisson distribution. The model is given by:

$$n_i = \beta_0 + \beta_1 d_i + \log(t_i) + \epsilon_i$$

where n_i is the number of days on which the i^{th} enrollee had an outpatient visit with the diagnosis code of interest, d_i takes the value of 1 if the enrollee was taking TZ/DZ/AZ or terazosin and 0 if the enrollee was taking tamsulosin, t_i is the total number of days the enrollee was taking that medication class, and $\epsilon_i$is a mean zero error term. The value of $\log(t_i)$ is included as an offset to account for different durations of observation between enrollees and is logged to match the link function expected by the quasi-Poisson distribution.

We elected to use a quasi-Poisson GLM over a classic Poisson GLM to allow for over-dispersion of the data. A Poisson distribution assumes that the mean and variance are equal. In practice, it is quite common for the variance of a count variable to be very different from the mean. The quasi-Poisson GLM extends the classic Poisson GLM by assuming that the variance can be written as the product of a scalar multiplier and the mean. This allows the data to have a larger variance than would be permitted under the classic Poisson framework.

We estimated relative risks for the 497 tested codes, 166 (33.4%) had a significantly different incidence between the groups at p=0.05. Of those, 43 (25.9%) were plausibly PD-related. The estimated relative risks for each of the 79 PD-related ICD-9 codes are shown in Table S1.

In the code-by-code model described above, we considered the incidence of each code separately and independently; however, there are clinically meaningful clusters of codes where pooling may increase the analytic power. The two neurologists labeled each PD related code as being a motor symptom, a non-motor symptom or a complication of PD and within those three large groups we further clustered codes into clinically meaningful groups or by organ system. We counted the number of days for each person where they had at least one of the codes in the sub-group and modeled this count using the same quasi-Poisson model described above. The relative risk for each of the main categories of PD-related diagnostic codes (motor, non-motor, and complications) and subgroups are listed in Table S2.

Incidence and Survival Analysis
A cohort of enrollees newly started on TZ/DZ/AZ or tamsulosin was constructed. We defined newly started as at least 365 days of enrollment with prescription drug coverage prior to the first fill event for TZ/DZ/AZ or tamsulosin. Additionally, we required the enrollee to be PD-free at the time of the first fill (no prior PD diagnosis code).

A total of 78,509 enrollees on TZ/DZ/AZ were identified and these enrollees were followed for an average of 285±382 days with a total of 118 cases of PD (incidence = 0.15%). We matched each TZ/DZ/AZ user to a tamsulosin user of the same age at medication start and with the minimum difference in the duration of followup. We were able to successfully match 78,444 of the 78,509 enrollees on TZ/DZ/AZ to an enrollee on tamsulosin. In the matched cohort, enrollees taking TZ/DZ/AZ have, on average, 284±381 days of followup compared to 284±382 days of follow up in those taking tamsulosin. Of the 78,444 enrollees taking TZ/DZ/AZ, a total of 118 (0.15%) developed PD compared to 190 (0.24%) among those taking tamsulosin.

We used a Cox proportional hazards regression to model the relative hazard of developing PD among those in the matched cohort taking TZ/DZ/AZ compared to those taking tamsulosin while accounting for censoring due to stopping the medication or exiting the data before developing PD. This model estimated a hazard ratio for those taking Az/Dz/Tz to be 0.62 (95% CI: 0.49-0.78).

Data availability.
Data and code for PPMI and Truven data are available at narayanan.lab.uiowa.edu/datasets.

Statistical and analysis considerations
For experiments to quantify animal behavior and for sample collections, experimenters were blinded to genotype and intervention, and studies were done by two different experimenters. Numbers of animals studied were based on our past experience and preliminary data. In all figures, data points are from individual mice and rats, or groups of flies. We did not exclude any data points from this study. Bars and whiskers indicate mean±SEM. Blue indicates controls and red indicates TZ treatment. Statistical significance for comparisons between data sets was

primarily with non-parametric tests. For studies of fly motor performance, our previous studies showed that within a group of flies (15-50 flies for one data point), the data fit a gaussian distribution. Moreover, multiple groups of flies also fit a gaussian distribution. Therefore, parametric tests were used to evaluate statistical significance. Table S5 shows the statistical test used for all data and the resulting P value for comparisons. All statistical tests were two-tailed. On individual graphs, we show statistical significance for the main comparisons with asterisks *$p<0.05$, **$p<0.01$, ***$p<0.001$.

REFERENCES

1. Liu ZY, Hu SP, Ji QR, Yang HB, Zhou DH, and Wu FF. Sevoflurane pretreatment inhibits the myocardial apoptosis caused by hypoxia reoxygenation through AMPK pathway: An experimental study. *Asian Pac J Trop Med.* 2017;10(2):148-51.
2. Chen HC, Lee JT, Shih CP, Chao TT, Sytwu HK, Li SL, et al. Hypoxia Induces a Metabolic Shift and Enhances the Stemness and Expansion of Cochlear Spiral Ganglion Stem/Progenitor Cells. *Biomed Res Int.* 2015;2015:359537.
3. Rockenstein E, Mallory M, Hashimoto M, Song D, Shults CW, Lang I, et al. Differential neuropathological alterations in transgenic mice expressing alpha-synuclein from the platelet-derived growth factor and Thy-1 promoters. *J Neurosci Res.* 2002;68(5):568-78.
4. Sonsalla PK, and Heikkila RE. The influence of dose and dosing interval on MPTP-induced dopaminergic neurotoxicity in mice. *Eur J Pharmacol.* 1986;129(3):339-45.
5. Paxinos G, and Watson C. The rat brain in stereotaxic coordinates. *Sydney Academic Press.* 1982.
6. Kirk D, Rosenblad C, and Björklund A. Characterization of behavioral and neurodegenerative changes following partial lesions of the nigrostriatal dopamine system induced by intrastriatal 6-hydroxydopamine in the rat. *Exp Neurol.* 1998;152(2):259-77.
7. Baluchnejadmojarad T, Roghani M, and Mafakheri M. Neuroprotective effect of silymarin in 6-hydroxydopamine hemi-parkinsonian rat: involvement of estrogen receptors and oxidative stress. *Neurosci Lett.* 2010;480(3):206-10.
8. Song L, Zhang Z, Hu R, Cheng J, Li L, Fan Q, et al. Targeting the D1-N-methyl-D-aspartate receptor complex reduces L-dopa-induced dyskinesia in 6-hydroxydopamine-lesioned Parkinson's rats. *Drug Des Devel Ther.* 2016;10:547-55.
9. Luchtman DW, Shao D, and Song C. Behavior, neurotransmitters and inflammation in three regimens of the MPTP mouse model of Parkinson's disease. *Physiol Behav.* 2009;98(1-2):130-8.
10. Laganiere J, Kells AP, Lai JT, Guschin D, Paschon DE, Meng X, et al. An engineered zinc finger protein activator of the endogenous glial cell line-derived neurotrophic factor gene provides functional neuroprotection in a rat model of Parkinson's disease. *J Neurosci.* 2010;30(49):16469-74.
11. Zhang FL, He Y, Zheng Y, Zhang WJ, Wang Q, Jia YJ, et al. Therapeutic effects of fucoidan in 6-hydroxydopamine-lesioned rat model of Parkinson's disease: Role of NADPH oxidase-1. *CNS Neurosci Ther.* 2014;20(12):1036-44.
12. Binley KE, Ng WS, Tribble JR, Song B, and Morgan JE. Sholl analysis: a quantitative comparison of semi-automated methods. *J Neurosci Methods.* 2014;225:65-70.
13. Tsui P, Telischi M, and Tsang VC. A rapid and economical method for the identification of anti-HIV antibodies by the western blot technique. *Biotechniques.* 1988;6(5):400-2.
14. Xu G, Xiong Z, Yong Y, Wang Z, Ke Z, Xia Z, et al. Catalpol attenuates MPTP induced neuronal degeneration of nigral-striatal dopaminergic pathway in mice through elevating glial cell derived neurotrophic factor in striatum. *Neuroscience.* 2010;167(1):174-84.
15. Liu L, and Duff K. A technique for serial collection of cerebrospinal fluid from the cisterna magna in mouse. *J Vis Exp.* 2008(21):pii: 960.
16. Quiros PM, Goyal A, Jha P, and Auwerx J. Analysis of mtDNA/nDNA Ratio in Mice. *Curr Proctoc Mouse Biol.* 2017;7(1):47-54.
17. Friggi-Grelin F, Coulom H, Meller M, Gomez D, Hirsh J, and Birman S. Targeted gene

expression in Drosophila dopaminergic cells using regulatory sequences from tyrosine hydroxylase. *J Neurobiol.* 2003;54(4):618-27.
18. Lee HT, Lin CS, Pan SC, Wu TH, Lees CS, Chang DM, et al. Alterations of oxygen consumption and extracellular acidification rates by glutamine in PBMCs of SLE patients. *Mitochondrion.* 2018;pii: S1567-7249(17):30195-2.
19. Sánchez-Danés A, Richaud-Patin Y, Carballo-Carbajal I, Jiménez-Delgado S, Caig C, Mora S, et al. Disease-specific phenotypes in dopamine neurons from human iPS-based models of genetic and sporadic Parkinson's disease. *EMBO Mol Med.* 2012;4(5):380-95.
20. Sánchez-Danés A, Consiglio A, Richaud Y, Rodríguez-Pizà I, Dehay B, Edel M, et al. Efficient generation of A9 midbrain dopaminergic neurons by lentiviral delivery of LMX1A in human embryonic stem cells and induced pluripotent stem cells. *Hum Gene Ther.* 2012;23(1):56-69.
21. Marek K, Jennings D, Lasch S, Siderowf A, Tanner C, Simuni T, et al. The Parkinson Progression Marker Initiative (PPMI). *Prog Neurobiol.* 2011;95(4):629-35.
22. Disease MDSTFoRSfPs. The Unified Parkinson's Disease Rating Scale (UPDRS): status and recommendations. *Mov Disord.* 2003;18(7):738-50.
23. Columbo JA, Kang R, Trooboff SW, Jahn KS, Martinez CJ, Moore KO, et al. Validating Publicly Available Crosswalks for Translating ICD-9 to ICD-10 Diagnosis Codes for Cardiovascular Outcomes Research. *Circ Cardiovasc Qual Outcomes.* 2018;11(10):e004782.
24. Raebel MA, Schmittdiel J, Karter AJ, Konieczny JL, and Steiner JF. Standardizing terminology and definitions of medication adherence and persistence in research employing electronic databases. *Med Care.* 2013;51(8 Suppl 3):S11-21.
25. https://www.ncpanet.org/pdf/adherence_list.pdf.
26. https://www.pqaalliance.org/adherence-measures.